Title: Measurement report: Long emission-wavelength chromophores dominate the light absorption of brown carbon in Aerosols over Bangkok: impact from biomass burning
Manuscript ID: acp-2021-175

Dear editor,

In compliance with the reviewers' detailed comments, we carefully revised the manuscript. We checked the text and references.

We appreciate the two reviewers for their helpful comments on our manuscript. We considered the detailed comments by the reviewers and responded to their suggestions and questions. For your and the reviewer's easiness to review the manuscript, an annotated manuscript was attached at the end of this file.

We are very sorry for making an error in the PMF model. We mistakenly brought the fluorescence of components of the 145-model into the PMF model, and the correct data should be that of the 85-model. Thus, we have revised it in the revised manuscript (Line 448–458).

We sincerely appreciate your consideration. Look forward to hearing from you soon.

With Best Regards,
Dr. Guangcai Zhong

Response to Anonymous Referee #1

RC- Reviewer's Comments; AC – Authors' Response Comments

RC1: This manuscript by Tang et al. represents a in-depth analysis of chromophores and fluorophores present in filter samples collected for an entire year in Bangkok. The authors use Excitation Emission Matrix, parafactor analysis (PARAFAC) and multiple linear regression (MLR) to provide insights into the contribution of potential sources to light absorbing organic compounds (BrC) in the samples collected. The chemical and data analyses were conducted with cautions. A year-round data from Bangkok serves as a precious case study for the community to understand light-absorbing organic compounds and their climate impact. I recommend publication in ACP after addressing the following minor comments.

AC1: Thanks for your recognition of our work and for providing valuable suggestions. We have made revisions following the comments (corrections are marked in the revised manuscript), and the responses are shown below.

RC2: Figure 1 - the color scale is not explained. Is it normalized to 1 for the highest intensity among all the factors?

AC2: We normalized to 0.1 for the highest intensity among all factors. We have added it as following: The color represents that the intensity was normalized to set the maximum as 0.1. Please see line 205-206 in the revised manuscript.

RC3: Figure 3 and related discussion. Although I agree with the authors in that the ratio of Abs365 and WSOC/MSOC is consistent, I also see that Abs365 is enhanced relative to WSOC/MSOC during the non-monsoon seasons. I wonder if the authors can investigate the ratios and discuss whether WSOC is more absorbing during BB-affected seasons?

AC3: We did see that the Abs_{365} is enhanced relative to WSOC/MSOC during the non-monsoon seasons. According to Table 1, the concentrations of levoglucosan that are generally regarded as biomass burning tracers were higher in the non-monsoon seasons than in monsoon season, and the ratios of levoglucosan/TSP also exhibited a similar trend (we have added the ratios in the revised manuscript, Table 1). Thus, we infer that the non-monsoon season was more affected by biomass burning. Correspondingly, both the WSOC and MSOC are more absorbing during the biomass burning-affected seasons (Table 1). Please see line 322-326 in the revised manuscript.

RC4: Line 387~ I think a little more discussions regarding the MLR results can be helpful for the community. Can the authors conclude that Abs365 in both WSOC and MSOC is dominated by a single factor (P4 for WSOC, C4 for MSOC). Is this result consistent with previous EEM and PARAFAC studies?

AC4: We have re-detailed the content of this part and please see line 411-419 in the revised manuscript. In this study, we attempted to build an MLR model to explore the relationship between the BrC absorption and fluorescent chromophores, and we thought that the coefficient (not a constant) in the equation represented the strength of the relationships. Thus, we can conclude that Abs_{365} is dominated by the single factor (P4 for WSOC, C4 for MSOC).

A similar study was conducted. Chen et al. (2019) thought that organic substances may represent the important causes of DTT (dithiothreitol) consumption and may be mainly contributed by light-absorbing materials. They found only two fluorescent components contribute to the DTT activity, almost all of which is attributed to the C7 chromophores with an emission wavelength of 462 nm (99%).

Reference:

Chen, Q., Wang, M., Wang, Y., Zhang, L., Li, Y., and Han, Y.: Oxidative Potential of Water-Soluble Matter Associated with Chromophoric Substances in PM2.5 over Xi'an, China, Environ. Sci. Technol., 53, 8574-8584, https://doi.org/10.1021/acs.est.9b01976, 2019.

RC5: Related to my previous comment, for WSOC, both P3 and P4 have an excitation maximum at around 365 nm. However, only P4 has a significant coefficient after MLR analysis. Meanwhile, P3 had a negative coefficient. Why is this?

AC5: In our MLR analysis, we set the constraints and manually selected regression model 3 for our optimal model. Regression model 4 is a calculation process and was also abandoned. However, the negative coefficient of P3 with Abs_{365} in regression model 4 could be due to the following reasons. First, from the mathematical meaning, in MLR analysis, simple correlation coefficients may not truly reflect the correlation between variables X and Y, because the relationship between variables is complex and they may be affected by more than one variable. Thus, the partial correlation coefficient is a better choice. In this study, to obtain the real correlation, we control the variables P4, P2, and P7 and make a correlation analysis between Abs_{365} and P3. The partial correlation analysis shows that Abs_{365} and P3 have a negative correlation (r=–0.227, Table A1), which is consistent with the negative coefficient in regression model 4. However, P3 does have an excitation at around 365 nm. According to the study of Phillips and Smith (2014), they explained that light absorption by organic aerosols is governed by a combination of independent as well as interacting chromophores. They introduce the charge transfer (CT) complexes as a significant source of BrC absorption, formed through the interaction between carbonyl and alcohol moieties in organic molecules, are energetically coupled to one another and form a near-continuum of states that absorb light from 250 to 600 nm, which may contribute up to 50% of light absorption (300–600nm) of the water-soluble fraction. In their experiment, they used $NaBH_4$ to individually reduce carbonyl functional groups in ketones and aldehydes, likely electron acceptors in CT complexes, to the corresponding alcohols. They observed that absorption spectra decrease and fluorescence increase of aqueous solutions after reduction by $NaBH_4$ (Phillips and Smith. 2015). This correlation between fluorescence gain and absorption loss demonstrates that the increased fluorescence is unlikely to result from newly created absorbing species and thus likely results from previously existing species that are more strongly fluorescing after reduction. Therefore, we infer that P3 likely a donor to interact with the other components to form CT complexes, resulting in increased absorption, but decreasing fluorescence due to the loss of functional groups. We hope the above points explain the reason that P3 has a negative coefficient with Abs_{365}.

Table A1. The partial correlation analysis between Abs_{365} and P3 under the control variables P2, P4, and P7.

Control variables			P3	Abs_{365}
P2 & P4 & P7	P3	*r*	1.000	-0.227
		p		0.040
	Abs_{365}	*r*	-0.227	1.000
		p	0.040	

References:

Phillips, S. M., and Smith, G. D.: Light Absorption by Charge Transfer Complexes in Brown Carbon Aerosols, Environ. Sci. Technol., 1, 382-386, https://doi.org/10.1021/ez500263j, 2014.

Phillips, S. M., and Smith, G. D.: Further evidence for charge transfer complexes in brown carbon aerosols from excitation-emission matrix fluorescence spectroscopy, J. Phys. Chem. A, 119, 4545-4551, https://doi.org/10.1021/jp510709e, 2015.

Response to Anonymous Referee #2

RC1: In this manuscript, the authors present a comprehensive study of water- and methanol-soluble chromophores and fluorophores in brown carbon (BrC) from aerosol samples collected year-round in Bangkok, using absorption and excitation-emission matrix (EEM) spectroscopies and numerical methods, including both parallel factor analysis (PMA) and positive matrix factorization (PMF). The selection and preparation of samples and the spectral and factor analyses are all well designed and carefully executed. The observations of chromophores and fluorophores together provide insights into the origin and fate of BrC in the atmosphere. For example, the PMA analysis of EEM observations indicates that atmospheric aging shifts the wavelengths of emission from fluorophores, as primary species react and secondary species form. The PMF analysis indicates that components most associated with absorption at 365 nm are largely emitted from biomass burning. These components are also characterized by long emission wavelengths, suggesting that the constituent molecules incorporate extended conjugated systems or charge-transfer interactions. With these and other impactful implications, the manuscript is suitable for publication in ACP. I have only technical and minor comments for the authors to consider.

AC1: We greatly appreciate the reviewer for recognizing the merits of this work and for providing valuable suggestions. These suggestions would help us improve the manuscript.

RC2: Line 31 - Please reword "these inferences exhibited a refutation".

AC2: Thanks for your suggestions, we have revised it as follows: which exhibited a different characteristic from primary biomass burning and coal combustion results. Please see line 31-32 in the revised manuscript.

RC3: Line 80 - Here and throughout the use of chromophore versus fluorophore is sometimes ambiguous. I would argue the claim in this sentence is not true, since many previous studies have explored the relationship between chromophores (i.e., the species that give a material its color) and BrC. If chromophores were to be replaced with fluorophores, or "fluorescent chromophores" as in line 94, the claim is not so problematic.

AC3: Thanks for your suggestions. We did confuse "fluorophore" and "chromophore". In the previous studies, for example, Lin et al. (2016, 2017, 2018) have investigated the relationship between chromophores and BrC using the combination of high-performance liquid chromatography (HPLC), photodiode array (PDA) spectrophotometry, and high-resolution mass spectrometry (HRMS). They identified BrC chromophores like polycyclic aromatic hydrocarbons (PAHs), heterocyclic O-PAHs and N-PAHs, nitro-phenols, et. The compounds can regard as chromophores. However, not all chromophores were fluorophores. In the study of Chen et al. (2019), they separately measured the light absorption and fluorescence properties of several nitrophenol standards, and the results showed strong light absorption properties, but no strong fluorescence signal was observed. Thus, we have replaced chromophores with "fluorescent chromophores" throughout the revised manuscript.

References:

Chen, Q., Mu, Z., Song, W., Wang, Y., Yang, Z., Zhang, L., and Zhang, Y. L.: Size - Resolved Characterization of the Chromophores in Atmospheric Particulate Matter From a Typical Coal - Burning City in China, J. Geophys. Res.-Atmos., 124, 10546-10563, https://doi.org/10.1029/2019jd031149, 2019.

Lin, P., Aiona, P. K., Li, Y., Shiraiwa, M., Laskin, J., Nizkorodov, S. A., and Laskin, A.: Molecular Characterization of Brown Carbon in Biomass Burning Aerosol Particles, Environ. Sci. Technol., 50, 11815-11824, https://doi.org/10.1021/acs.est.6b03024, 2016.

Lin, P., Bluvshtein, N., Rudich, Y., Nizkorodov, S. A., Laskin, J., and Laskin, A.: Molecular Chemistry of Atmospheric Brown Carbon Inferred from a Nationwide Biomass Burning Event, Environ. Sci. Technol., 51, 11561-11570, https://doi.org/10.1021/acs.est.7b02276, 2017.

Lin, P., Fleming, L. T., Nizkorodov, S. A., Laskin, J., and Laskin, A.: Comprehensive Molecular Characterization of Atmospheric Brown Carbon by High Resolution Mass Spectrometry with Electrospray and Atmospheric Pressure

Photoionization, Anal. Chem., 90, 12493-12502, https://doi.org/10.1021/acs.analchem.8b02177, 2018.

RC4: Line 112 - Include units of electrical resistivity.

AC4: We have added the units of electrical resistivity (resistivity of > 18.2 MΩ) in the revised manuscript. Please see line 114 in the revised manuscript.

RC5: Line 113 - Replace "GFFs" with "QFFs".

AC5: Thanks for your revision, we have revised it.

RC6: Line 213 - Please consider rephrasing the sentence beginning with "Although one exceptional component was detected..." The meaning is not clear to me.

AC6: In this part, we wanted to express that one additional fluorescent component was identified in the new 145-model (the model contains the total EEMs of 60-sources samples and 85-Thailand TSP samples) for WSOC and MSOC fraction comparing with the 85-model (the model only contains the EEMs of 85-Thailand TSP samples), respectively. Now, we have revised the sentence as follows: It should be noted that one additional fluorescent component was identified each for the WSOC and MSOC fractions in the new 145-model, respectively, but these components were only highly characterized by source emission samples. Please see line 219-224 in the revised manuscript.

RC7: Line 335 - Mention the range of measured pH values.

AC7: The pH values of WSOC fraction for all the samples were within the range of 5–7, generally thinking it didn't affect the absorbance according to a prior study (Chen et al., 2016). We have added it, please see line 350-351 in the revised manuscript.

Reference:

Chen, Q., Ikemori, F., and Mochida, M.: Light Absorption and Excitation-Emission Fluorescence of Urban Organic Aerosol Components and Their Relationship to Chemical Structure, Environ. Sci. Technol., 50, 10859-10868, https://doi.org/10.1021/acs.est.6b02541, 2016.

RC8: Line 341 - I am surprised by how much more absorptive the WSOC is than the MSOC. Can comparisons also be made for specific periods dominated by biomass burning emissions, identified using the PMF analysis or even simply the MODIS active fire spots? I would expect MSOC to be significantly more absorptive than WSOC during these periods.

AC8: We observed that WSOC were more absorption than the MSOC in our study. We also check the biomass burning-impacted periods by the biomass burning tracer level (i.e., levoglucosan concentration and the ratio of levoglucosan/TSP, see Table 1),

whereas WSOC is still more absorption than MSOC. Similarly, Bikkina et al. (2020) observed that the marine-impacted aerosols of the Bay of Bengal showed higher MAE_{365} values in the WSOC fraction than MSOC fraction (only extract using methanol), and they explained it due to two plausible reasons. First, the BrC aerosols over Bay of Bengal have a contribution from a different source (i.e., maritime influence) and contain BrC-chromophores that are more soluble in water than methanol. Secondary, there could be significant photobleaching effects of different chromophores. However, Kim et al. (2016) reported that the light absorption contributed by water-insoluble organic carbon (WISOC) exhibited a clear seasonal variation in Seoul, with the strong light absorption contributed by WISOC in summer, while WSOC was the main contributor in the other seasons. They attributed it to that photochemically generated secondary organic aerosols from anthropogenic emissions seem to be the main source in summer, whereas aged/oxidized compounds were the main source in the other seasons. Thus, we infer that the different sources and atmospheric processes would impact the distribution of WSOC and WISOC fractions.

Also, laboratory experiment shows that intermediate relative humidity (55–65%) promoted secondary BrC formation (Kasthuriarachchi et al., 2020). Considering the high temperature and humidity (Table S1), high WSOC/OC ratios (50%±9.9%), and tropical monsoon climate in Thailand, it would promote more water-soluble chromophores over Thailand. The modified part is in the line 363-373 in the revised manuscript.

References:

Bikkina, P., Bikkina, S., Kawamura, K., Sudheer, A. K., Mahesh, G., and Kumar, S. K.: Evidence for brown carbon absorption over the Bay of Bengal during the southwest monsoon season: a possible oceanic source, Environ Sci Process Impacts, 22, 1743-1758, https://doi.org/10.1039/d0em00111b, 2020.

Kasthuriarachchi, N. Y., Rivellini, L.-H., Chen, X., Li, Y. J., and Lee, A. K. Y.: Effect of relative humidity on secondary brown carbon formation in aqueous droplets, Environ. Sci. Technol., 54, 13207-13216, https://doi.org/10.1021/acs.est.0c01239, 2020.

Kim, H., Kim, J. Y., Jin, H. C., Lee, J. Y., and Lee, S. P.: Seasonal variations in the light-absorbing properties of water-soluble and insoluble organic aerosols in Seoul, Korea, Atmos. Environ., 129, 234-242, https://doi.org/10.1016/j.atmosenv.2016.01.042, 2016.

RC9: Line 343 - On a similar note, here or in Section 2.1, please clarify how MSOC was prepared. Was it extracted from nascent filters or filters already extracted with water? If the latter, "MSOC" is perhaps inaccurate since many methanol-soluble

compounds will have already been extracted into water, and it could be more precise to refer to MSOC as water-insoluble BrC throughout.

AC9: Thanks for your suggestions. MSOC in this study is the latter, which was extracted using methanol from filters already extracted with water. According to the previous studies (Liu et al., 2013; Shetty et al., 2019), only water cannot effectively extract the BrC constituent, and the remaining part of the filter is water-insoluble fraction. To understand the optical characteristics of these water-insoluble materials, the remaining filter extracted after purified water was further freeze-dried and extracted with methanol to obtain the MSOC. We have clarified it and please see line 115-117 in the revised manuscript.

The reason that we choose "MSOC" to represent the methanol-extracted organic fraction in this study is that methanol could not completely extract these substances which cannot dissolve in water. Further, we wanted to make a comparison with the result of our previous study with a similar extraction method (Tang et al., 2020). Similarly, Chen et al. (2019) also used "WSM" to represent the water-soluble matter and "MSM" represent the methanol-soluble matter in the same manner as our extraction method.

References:

Chen, Q., Mu, Z., Song, W., Wang, Y., Yang, Z., Zhang, L., and Zhang, Y. L.: Size‐Resolved Characterization of the Chromophores in Atmospheric Particulate Matter From a Typical Coal‐Burning City in China, J. Geophys. Res.-Atmos., 124, 10546-10563, https://doi.org/10.1029/2019jd031149, 2019.

Liu, J., Bergin, M., Guo, H., King, L., Kotra, N., Edgerton, E., and Weber, R. J.: Size-resolved measurements of brown carbon in water and methanol extracts and estimates of their contribution to ambient fine-particle light absorption, Atmos. Chem. Phys., 13, 12389-12404, https://doi.org/10.5194/acp-13-12389-2013, 2013.

Shetty, N. J., Pandey, A., Baker, S., Hao, W. M., and Chakrabarty, R. K.: Measuring light absorption by freshly emitted organic aerosols: optical artifacts in traditional solvent-extraction-based methods, Atmos. Chem. Phys., 19, 8817-8830, https://doi.org/10.5194/acp-19-8817-2019, 2019.

Tang, J., Li, J., Su, T., Han, Y., Mo, Y., Jiang, H., Cui, M., Jiang, B., Chen, Y., Tang, J., Song, J., Peng, P., and Zhang, G.: Molecular compositions and optical properties of dissolved brown carbon in biomass burning, coal combustion, and vehicle emission aerosols illuminated by excitation–emission matrix spectroscopy and Fourier transform ion cyclotron resonance mass spectrometry analysis, Atmos. Chem. Phys., 20, 2513-2532, https://doi.org/10.5194/acp-20-2513-2020, 2020.

RC10: Line 383 - I think it is important to mention this point, that not all chromophores in BrC are fluorophores, in the introduction.

AC10: Many thanks for your suggestions, we have added this point in the introduction. Please see line 80-81 in the revised manuscript.

RC11: Line 420 - Perhaps discuss Figures S15-16 here as corroborating evidence for the importance of biomass burning.

AC11: Here we made an error previously. We mistakenly brought the fluorescence intensity of components of the 145-model into the PMF model, and the correct data should be that of the 85-model. Thus, we revised it in the revised manuscript and there were slightly different source-contribution from the previous. Further, to more detailly explain the importance of biomass burning, we added the time-series of light absorption and fluorescence components contributed by different sources resolved by the PMF model (Figure 6 and Figure S15). The biomass burning contribution for BrC absorption at 365 nm, and P4 and C4 components is reduced in the monsoon season. Combining the fire spots and backward trajectory (Figure S16-S17), the time series of source contribution points out that high biomass burning contribution is related to the higher local fire spots (i.e., pre-hot season, hot season, and cool season) and air mass from the continent. Jiang et al. (2021) observed increases in biomass burning contributions to BrC absorption during the winter period that was dominant in continental-origin air masses. We have added more discussion in this part (line 448-458) in the revised manuscript.

Reference:

Jiang, H., Li, J., Sun, R., Liu, G., Tian, C., Tang, J., Cheng, Z., Zhu, S., Zhong, G., Ding, X., and Zhang, G.: Determining the Sources and Transport of Brown Carbon Using Radionuclide Tracers and Modeling, J. Geophys. Res.-Atmos., 126, https://doi.org/10.1029/2021jd034616, 2021.

Measurement report: Long emission-wavelength chromophores dominate the light absorption of brown carbon in Aerosols over Bangkok: impact from biomass burning

Jiao Tang[1,2,3], Jiaqi Wang[1,2,3,7], Guangcai Zhong[1,2,3], Hongxing Jiang[1,2,3,7], Yangzhi Mo[1,2,3], Bolong Zhang[1,2,3,7], Xiaofei Geng[1,2,3,7], Yingjun Chen[4], Jianhui Tang[5], Congguo Tian[5], Surat Bualert[6], Jun Li[1,2,3], Gan Zhang[1,2,3]

[1]State Key Laboratory of Organic Geochemistry and Guangdong Key Laboratory of Environmental Protection and Resources Utilization, Guangzhou Institute of Geochemistry, Chinese Academy of Sciences, Guangzhou 510640, China

[2]CAS Center for Excellence in Deep Earth Science, Guangzhou, 510640, China

[3]Joint Laboratory of the Guangdong-Hong Kong-Macao Greater Bay Area for the Environment, Guangzhou Institute of Geochemistry, Chinese Academy of Sciences, Guangzhou 510640, China

[4]Department of Environmental Science and Engineering, Fudan University, Shanghai 200092, P.R. China

[5]Key Laboratory of Coastal Environmental Processes and Ecological Remediation, Yantai Institute of Coastal Zone Research, Chinese Academy of Sciences, Yantai 264003, China

[6]Faculty of Environment, Kasetsart University, Bangkok, 10900, Thailand

[7]University of Chinese Academy of Sciences, Beijing 100049, China

Correspondence: Guangcai Zhong (gczhong@gig.ac.cn)

Abstract: Chromophores represent an important portion of light-absorbing species, i.e. brown carbon. Yet knowledge on what and how chromophores contribute to aerosol light absorption is still sparse. To address this problem, we examined soluble independent chromophores in a set of year-round aerosol samples from Bangkok. The water-soluble fluorescent chromophores identified via excitation-emission matrix (EEM) spectroscopy and follow-up parallel factor analysis could be mainly assigned as humic-like substances and protein-like substances, which differed in their EEM pattern from that of the methanol-soluble fraction. The emission wavelength of fluorescent chromophores in environmental samples tended to increase compared with that of the primary combustion emission, which could be attributed to secondary formation or the aging process. Fluorescent indices inferred that these light-absorbing chromophores were not significantly humified and comprised a mixture of organic matter of terrestrial and microbial origin, ~~while~~ which exhibited a different characteristic ~~these inferences exhibited a refutation with~~ from primary biomass burning and coal combustion results. A multiple linear regression analysis revealed that larger fluorescent chromophores that were oxygen-rich and highly aromatic with high molecular weights, were the key contributors of light absorption, preferably at longer emission wavelength (λ_{max} > 500 nm). Positive matrix factorization analysis further suggested that up to ~~60~~50% of these responsible chromophores originated from biomass burning emissions.

1. Introduction

Atmospheric aerosols play a substantial role in climate change through radiative forcing (Alexander et al., 2008). Carbonaceous aerosols mainly include organic carbon (OC) and elemental carbon (EC). Brown carbon (BrC) is a specific type of OC that absorbs radiation efficiently in the near-ultraviolet and visible (UV-vis) range (Laskin et al., 2015;Kirchstetter et al., 2004) and may contribute 15% or more of total light absorption over the UV-vis spectrum (Kirchstetter and Thatcher, 2012;Liu et al., 2013). This fraction can significantly affect atmospheric chemistry, air quality, and climate change (Marrero-Ortiz et al., 2018;Laskin et al., 2015). Forest fires, residential heating by wood and coal, biogenic release, and secondary formation contribute to BrC in the atmosphere (Laskin et al., 2015). Many studies have indicated that the optical properties of BrC may significantly evolve as a result of atmospheric processes such as oxidation (Fan et al., 2020), solar irradiation (Wong et al., 2017), and relative humidity (Kasthuriarachchi et al., 2020). These factors cause variability in the chemical compositions and levels of BrC across source regions and receptors, resulting in a high degree of uncertainty regarding the effects of BrC (Dasari et al., 2019;Xie et al., 2019).

Light absorption of BrC is associated with its molecular composition and chemical structure (Song et al., 2019;Lin et al., 2018;Mo et al., 2018;Jiang et al., 2020). Detailed structural characterization of BrC compounds is essential to understand their sources and chemical processes in the atmosphere. High-resolution mass spectrometry (HRMS) is a powerful tool for molecular-level chemical analysis of organic aerosols (Laskin et al., 2018). Combinations of offline high-performance liquid chromatography (HPLC), a photodiode array detector, and HRMS allow the chemical characterization of aerosols specific to BrC (Lin et al., 2018;Lin et al., 2016;Lin et al., 2015;Lin et al., 2017). With these combination approaches, nitroaromatics, aromatic acids, phenols, polycyclic aromatic hydrocarbons and their derivatives are basically identified as BrC chromophores (Wang et al., 2020b;Yan et al., 2020). However, it should be noted that it is difficult to ionize some organic compounds for detection using HRMS, and even for those that can be detected, HRMS can only provide possible molecular structures based on empirical deduction (Song et al., 2018;Lin et al., 2015). The isomeric complexity of natural organic matter may have exceeded achievable one-dimensional chromatographic resolution (Hawkes et al., 2018), and therefore, the majority of components in the BrC mixture remain undetermined.

Excitation-emission matrix (EEM) fluorescence spectroscopy detects bulk chromophores in a solution (Chen et al., 2016b). Chromophores can be revealed by EEM with information on their chemical structures associated with molecular weight, aromatic rings, conjugated systems, etc (Wu et al., 2003). For example, a redshift in emission spectral maxima can be caused by an increase in the

number of aromatic rings condensed in a straight chain, conjugated double bonds, or formational changes that permit vibrational energy losses of the promoted electrons (Wu et al., 2003). A significant Stokes shift with emission wavelength can be observed in aged secondary organic aerosols (SOA) using EEM spectroscopy (Lee et al., 2013). Parallel factor (PARAFAC) analysis has been widely used to decompose the EEM spectral signature into independent underlying components (Han et al., 2020;Yue et al., 2019;Wu et al., 2019;Chen et al., 2019b), adding valuable information to absorbance-based measurements (Yan and Kim, 2017). This technique helps to categorize groups of similar fluorophores or chromophores or similar optical properties, thereby allowing a better understanding of the chemical properties of BrC, while it should be noted that not all chromophores in BrC compounds are fluorescence (Chen et al., 2019a). There is evidence that BrC absorption is closely correlated with fluorescent chromophores (Huo et al., 2018). However, the intrinsic relationship between fluorescent chromophores and BrC absorption has not been explored.

Southeast Asia is subject to intensive regional biomass burning, the emissions from which may contribute to atmospheric brown clouds (Ramanathan et al., 2007;Laskin et al., 2015). The contribution of biomass burning to aerosol optical depth was evaluated to be more than 56% over this region (Huang et al., 2013). Despite many studies focused on the characterization of atmospheric black carbon (BC) (See et al., 2006;Fujii et al., 2014;Permadi et al., 2018), studies on BrC in the region are still limited. A recent study in Singapore indicated that water-soluble OC (WSOC) exhibited strong wavelength dependence and even higher values of BrC absorption than those from Korea, India, China, and Nepal (Adam et al., 2020), indicating abundant water-soluble BrC in the air over Southeast Asia.

This study was performed to explore the relationships between EEM chromophores and BrC light absorption in soluble aerosol organic matter. A set of year-round aerosol samples from Bangkok, Thailand, was analyzed. Water-soluble and methanol-soluble BrC in the aerosol samples were characterized by EEM followed by statistical analyses to retrieve information on the contributions of fluorescent chromophores to BrC light absorption, as well as their emission sources. This study provides a comprehensive dataset on seasonal variability in the light absorption properties, sources, and chemical components of BrC, which may be useful for improving further modeling and field observation.

2. Experiment

2.1. Sample Collection and Extraction.

Eighty-five total suspended particulate (TSP) samples were collected on the roof (57 m above ground level) of the Faculty of Environment, Kasetsart University (100°57′ E and 13°85′ N) in Bangkok, Thailand (Fig. S1). Detailed information about the sampling site is presented elsewhere

(Wang et al., 2020a). Sampling was performed from January 18, 2016 to January 28, 2017, and the sampling period was divided into four seasons: the pre-hot season (January 18–February 28, 2016), hot season (March 2–May 30, 2016), monsoon (June 2–October 30, 2016), and cool season (November 1, 2016–January 28, 2017). Table S1 lists the average meteorological data in the four seasons. Generally, during the sampling period, the hot season was characterized by high temperatures and wind speeds, and the monsoon season by high humidity. TSP samples were collected over 24 h using a high-volume (0.3 m^3 min^{-1}) sampler with quartz-fiber filters (QFFs, prebaked for 6 h at 450 °C). All samples and field blanks were stored under dark conditions at –20 °C until analysis.

WSOC was prepared by ultrasonication extraction of filter punches with ultra-pure deionized water (resistivity of > 18.2 MΩ~~Ω > 18.2~~). The methanol-soluble OC (MSOC) fraction was then obtained by extracting the freeze-dried residue on the same ~~GFFs~~ QFFs after water extraction with HPLC-grade methanol, which is used for water-insoluble fractions (Chen and Bond, 2010). It is worth noting that the MSOC in this study is not necessarily like that of the same name in other studies. The extract solutions were passed through 0.22-μm PTFE filters and subjected to follow-up UV-vis absorption and fluorescence spectral analysis. The mass concentrations of WSOC and MSOC were measured, and the method are shown in the Supplement.

2.2. Absorption Spectra and Fluorescence Spectra.

The extract solutions were placed in quartz cells with a path-length of 1 cm and subjected to analysis using an fluorometer (Aqualog; Horiba Scientific, USA). Absorption spectra and EEM spectra were obtained simultaneously using this instrument. The contribution of solvents was subtracted from the extract spectra. UV-vis absorption spectra were scanned in the range of 239 to 800 nm with a step size of 3 nm. The Fluorescence spectra were recorded with emission wavelength (Em) ranging from 247.01 to 825.03 nm and excitation wavelength (Ex) ranging from 239 to 800 nm. The wavelength increments of the scans for Em and Ex were 4.66 and 3 nm, respectively. The calculation of optical parameters and the relative contributions of BrC to total aerosol light absorption are presented in the Supplement.

2.3. Factor analysis

In this study, we built a PARAFAC model, based on 85 TSP sample fluorescence (samples × Ex × Em: 85 × 188 × 125, 85-model). Original EEM spectra were corrected and decomposed via PARAFAC analysis with reference to earlier methods using drEEM toolbox version 2.0 with MATLAB software (http://models.life.ku.dk/drEEM, last access: June 2014) (Murphy et al., 2013;Andersson and Bro, 2000). The absorbance, all below 1 at 239 nm, was deemed suitable for correcting the EEM

spectra for inner filter effects (IFEs) (Luciani et al., 2009;Gu and Kenny, 2009;Fu et al., 2015), and the sample EEM spectra, and blanks were normalized relative to the Raman peak area of ultrapure deionized water collected on the same day to correct fluorescence in Raman Units (RU) (Murphy et al., 2013;Murphy et al., 2010). Spectra with Em > 580 nm and Ex < 250 nm were removed to eliminate noisy data. The non-negativity constraint is necessary to obtain reasonable spectra, and signals of first-order Rayleigh, Raman, and second-order Rayleigh scattering in the EEM spectra were removed using the interpolation method (Bahram et al., 2006). The two- to nine-component PARAFAC model was explored, within the context of spectral loading, core consistency, and residual analysis (Figs. S2–S5). Finally, seven and six components were identified in the WSOC and MSOC fractions, which explained 99.89% and 99.76% of the variance, respectively. Both the seven- and six-component PARAFAC solutions passed the split-half analysis with the split style of "$S_4C_6T_3$", and residuals were examined to ensure that there was no systematic variation. The parameters obtained from the PARAFAC model were used to calculate the approximate abundance of each component, expressed as F_{max} (in RU), corresponding to the maximum fluorescence intensity for a particular sample.

Fluorescence indices based on intensity ratios that provide insight into the origins of dissolved BrC, such as the humification index (HIX) (the ratio of average emission intensity in the 435−480-nm range to that in the 300−345-nm range following excitation at 254 nm, which was used to reflect the degree of humification) (Zsolnay et al., 1999), the biological index (BIX) (the ratio of emission intensities at 380 and 430 nm following excitation at 310 nm, reflecting autochthonous biological activity in water samples) (Huguet et al., 2009), and fluorescence index (FI) (the ratio of emission intensities at 470 and 520 nm following excitation at 370 nm, reflecting the possibility of microbial origin and for examining differences in precursor organic materials) (Lee et al., 2013;Murphy et al., 2018).

2.4. Statistical analysis

A hierarchical cluster method was used to classify aerosol samples based on the relative contributions of PARAFAC components to the respective samples. The Squared Euclidean distance method was used to evaluate the distances between samples, and the Between-group linkage method was chosen for hierarchical cluster analysis. The multiple linear regression (MLR) model was applied to elucidate the relationship between fluorescent chromophores and light absorption of BrC using a stepwise screening process. Analyses were performed using SPSS software (SPSS Inc., Chicago, IL, USA).

3. Results and Discussion

3.1. EEM of dissolved organic substances.

Fluorescence spectra coupled with PARAFAC results can provide more information about the chemical structures of chromophores. Figure 1 and Table S2 show the seven-component (P1–7) PARAFAC solutions of WSOC in the samples of aerosol over Bangkok, the peaks of which fell mainly into the humic-like and protein-like chromophore regions in the plots. Components P2, P3, P4, and P6 were identified as humic-like substances (HULIS) (Chen et al., 2017a;Stedmon and Markager, 2005;Wu et al., 2019;Chen et al., 2003). A second peak was observed at a high excitation wavelength for these components, indicating the existence of a large number of condensed aromatic moieties, conjugated bonds, and nonlinear ring systems (Matos et al., 2015). Among them, P2, P3, and P4 had a longer emission wavelength (> 400 nm) than P6, likely due to the low probability of fluorescence emission from quinonoid n-π* transitions (Cory and McKnight, 2005). P3 produced similar spectra to those of aqueous reaction products of hydroxyacetone with glycine (Gao and Zhang, 2018), and dissolved organic matter (DOM) in the surface water of Xiangxi Bay and Three Gorges Reservoir (Wang et al., 2019). P6 had a peak similar to those in the fluorescence spectra of N-containing SOA species formed by α-pinene under ozonolysis and photooxidation with NH_3 in a flow reactor (Babar et al., 2017) as well as pyridoxine (Pohlker et al., 2012), indicating a possible biological source. P5 was similar to a previously identified fluorophore in $PM_{2.5}$ from Xi'an (Chen et al., 2019b). P1 and P7 could be assigned as protein-like organic matter (PLOM) due to their short emission wavelengths (Wu et al., 2003). Specifically, P7 resembled a tyrosine-like fluorophore (Zhou et al., 2019;Chen et al., 2003) and may be related to non-N-containing species (Chen et al., 2016b).

The MSOC fraction extracted from the filter residue after water extraction produced fluorescence signals with fluorescence patterns different from those of the WSOC fraction, indicating a different chemical composition from that of WSOC. Thus, WSOC with the addition of MSOC may provide a more comprehensive description of the optical and chemical characteristics of BrC compared to WSOC alone. Six components (C1–C6) were resolved for the MSOC. Among them, C1 and C2 were associated with shorter excitation wavelengths (< 250 nm) but longer emission wavelengths (> 380 nm), indicating the presence of fulvic-like substances (Chen et al., 2003;Mounier et al., 1999). C6 produced a pattern similar to that of tyrosine-like fluorescence (Stedmon and Markager, 2005). Although C4 had a similar EEM spectrum as P4 of WSOC, the two components were chemically different in polarity, suggesting different behaviors in the environment (Ishii and Boyer, 2012). Note that there were no special chemical structures for the different types of chromophores, and therefore, the origins and chemical structures of HULIS and PLOM studied here are not necessarily like those with the same names in other types of organic matter.

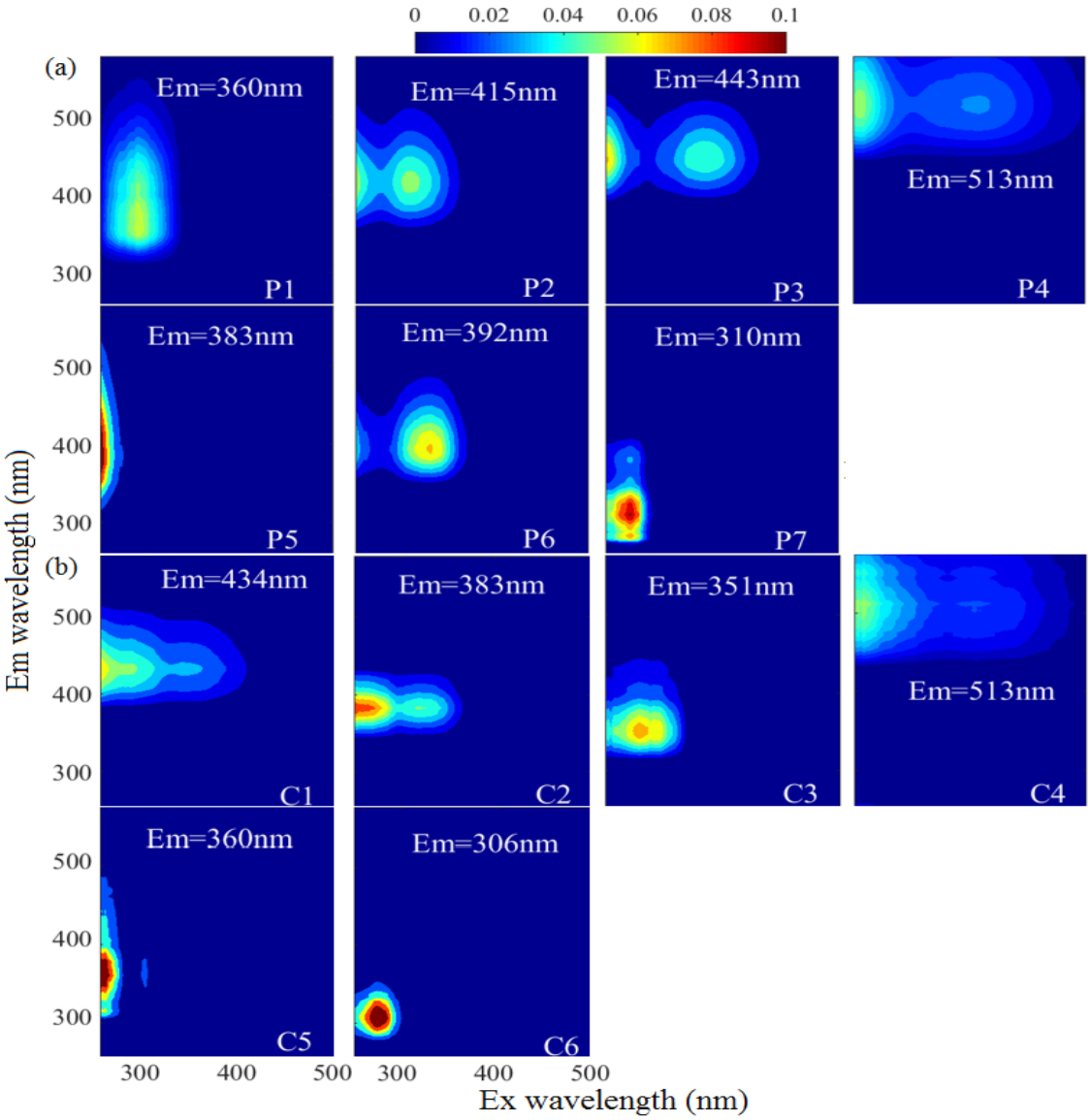

Figure 1. The fluorescent components identified by the PARAFAC (parallel factor) analysis for EEM of water-soluble organic carbon (P1–P7, WSOC, a) and methanol-soluble organic carbon (C1–C6, MSOC, b) in the aerosol samples over Bangkok in Thailand (n=85). The color represents that the intensity was normalized to set the maximum as 0.1.

To further explore the potential sources of the EEM-PARAFAC components, we added 60 source samples to the matrices. The source sample EEM data were described in our previous study (Tang et al., 2020b), including those of 33 biomass-burning samples (IDs: 1–33), 17 coal-combustion samples (IDs: 34–50) samples, eight tunnel samples (IDs: 51–58) and two vehicle-exhaust samples from trucks (IDs: 59–60) , which are important sources of BrC in the atmosphere. This, in combination with our Bangkok field samples, yielded a new matrix (145 × 188 × 125, 145-model) for modeling. PARAFAC analysis successfully decomposed the dataset, and the output was the same as for the 85-model. The component solutions are presented in Fig. S6. To validate the stability of the model after loading by the new matrix, the Tucker congruence coefficient (TCC) was calculated to determine the similarity

of two fluorescence spectra between the two models (refer to Text S3 of Supplement). Note that a higher TCC value would indicate a higher degree of similarity of the spectra. As shown in Table S2 and Fig. S7, high TCC values were found as expected between the 85-model components and the 145-model components, indicating that the two models identified similar fluorescent chromophores. It should be noted that one additional fluorescent component was identified each for the WSOC and MSOC fractions in the new 145-model, respectively, but these components were only highly characterized by source emission samples,~~Although one exceptional component was detected each for the WSOC and MSOC fractions by the new 145-model, these fluorescent components were only highly characterized by source samples,~~ as reported in our previous study (Tang et al., 2020b).

Using the distribution proportions of the EEM-PARAFAC fitted components (145-model), we conducted hierarchical cluster analysis of the mixed ambient and source samples. The results are shown in Figs. S9 and S10. For the WSOC fraction, all aerosol samples from Bangkok and tunnel samples were assigned to cluster A, whereas biomass-burning and coal-combustion aerosols were assigned to clusters C and D, respectively. This implied that the fluorescent chromophore types could be somewhat related to the emission precursors of the aerosol components. However, the distribution of fluorescent chromophores varied clearly between the ambient aerosols and source samples. The ambient aerosol samples contained higher levels of fluorescent chromophores with longer emission wavelengths that were related to humic-like or fulvic-like chromophores (components 145M-P1 (P1 component in 145-model), 145M-P5, and 145M-P6), whereas the primary biomass-burning and coal-combustion samples contained high-intensity fluorescent chromophores with shorter emission wavelengths that were related to protein-like fluorescence (145M-P2 and 145M-P4). These phenomena was similarly reported previously, i.e., protein-like substances produce compounds with similar fluorescence properties as humic substances under irradiation conditions (Bianco et al., 2014). Similar differences between field samples and source samples were found for the MSOC fraction. Therefore, our results confirmed that chemical reactions or "aging" in the atmosphere greatly modifies the chromophore patterns of emission sources by both bleaching the source chromophores or producing new chromophores and, at least in this case, shifts the chromophore emission wavelength toward longer wavelengths, i.e., from protein-like to fulvic-like (Bianco et al., 2014;Bianco et al., 2016;Lee et al., 2013).

3.2. Fluorescence-derived indices

The ratios of fluorescence intensity from specific spectral regions of an EEM were used as indicators for the relative contributions of organic matter derived from terrestrial or microbial sources in natural waters (Shimabuku et al., 2017;Birdwell and Engel, 2010;Mcknight et al., 2001). HIX was

initially introduced to estimate the degree of maturation of DOM in soil (Zsolnay et al., 1999), representing the degree of humification of organic matter, for which higher HIX values also indicate higher degree of polycondensation (low H/C ratio) and aromaticity (Qin et al., 2018). Generally, high HIX values (> 10) correspond to strongly humified or aromatic organics, principally of terrestrial origin, whereas low values (< 4) are indicative of autochthonous or microbial origin. As shown in Table 1 and Fig. 2, the HIX values were 3.4±0.99 and 2.0±0.59 for WSOC and MSOC, respectively, in aerosol samples from Bangkok. All HIX values were less than 10, which could be viewed as a nominal cutoff below which DOM is not significantly humified (Birdwell and Valsaraj, 2010;Zsolnay et al., 1999;Huguet et al., 2009). Figure 2 shows the HIX values in primary biomass-burning and coal-combustion samples, which were much lower than those in the ambient samples, indicating that the lower values of HIX in the atmosphere likely correspond to freshly introduced material. Lee et al. (2013) reported that fresh SOA had low HIX values, but these values increased significantly upon aging with ammonia. The much higher HIX values in the WSOC compared to the MSOC suggest that WSOC may have a higher degree of aromaticity or a more condensed chemical structure. Our previous study revealed that MSOC has a higher molecular weight but lower aromaticity index than the corresponding WSOC in combustion experiment aerosol samples, indicating a more aliphatic structure in the MSOC (Tang et al., 2020b). The HIX values of WSOC were highest in the hot season (3.9±1.1), followed by the pre-hot season (3.3±1.1), cool season (2.9±0.36), and monsoon (2.5±0.22), whereas those of the MSOC tended to be higher in the hot and cool seasons than in the monsoon and pre-hot seasons. The HIX values in the WSOC fraction were comparable to those of water-soluble organic aerosols in the high Arctic atmosphere (mean: 2.9) (Fu et al., 2015) and higher than those of water-soluble aerosols (1.2±0.1 in winter and 2.0±0.3 in summer) over northwest China (Qin et al., 2018), likely indicating a higher degree of chromophore humification.

Table 1 Seasonal averages of the concentration of organic carbon (OC), elemental carbon (EC), water-soluble organic carbon (WSOC), and methanol-soluble organic carbon (MSOC), BrC absorption, fluorescence indices and levoglucosan level for aerosol samples collected from Bangkok in Thailand. Pre-hot season is from January 18 to February 29, 2016; hot season is from March 2 to May 31, 2016; monsoon is from June 2 to October 30, 2016; cool season is from November 1, 2016 to January 28, 2017.

	Annual (n=85) Ave ± sd	Pre-Hot season (n=7) Ave ± sd	Hot season (n=41) Ave ± sd	Monsoon (n=7) Ave ± sd	Cool season (n=30) Ave ± sd
[a]OC (μg C m^{-3})	12±7.3	19±9.3	9.6±6.7	6.5±0.97	16±5.6
[a]EC (μg C m^{-3})	1.4±0.48	2.0±0.45	1.2±0.47	1.2±0.15	1.5±0.40
[a]OC/EC	8.9±5.2	9.6±3.4	8.4±6.8	5.4±0.51	10±2.5

			WSOC		
μg C m^{-3}	6.2±4.2	9.9±5.7	5.3±4.1	2.6±0.31	7.4±3.4
AAE (330–400 nm)	5.1±0.68	5.0±0.52	5.4±0.56	6.2±0.11	4.5±0.34
Abs_{365} (Mm^{-1})	5.6±4.9	10±7.4	4.5±4.5	1.2±0.21	7.2±4.1
MAE_{365} (m^2 g^{-1} C)	0.83±0.25	0.96±0.19	0.78±0.23	0.45±0.06	0.95±0.21
FI	1.6±0.10	1.6±0.09	1.6±0.08	1.7±0.07	1.7±0.07
BIX	0.82±0.13	0.83±0.14	0.74±0.13	0.92±0.05	0.89±0.07
HIX	3.4±0.99	3.3±1.1	3.9±1.1	2.5±0.22	2.9±0.36
			MSOC		
μg C m^{-3}	6.0±3.4	9.2±4.0	4.3±2.9	3.9±0.86	8.1±2.6
AAE (330–400 nm)	5.2±0.94	4.9±0.69	5.5±1.1	5.1±0.15	4.7±0.55
Abs_{365} (Mm^{-1})	1.7±1.4	1.9±1.6	1.0±0.99	0.72±0.23	2.7±1.4
MAE_{365} (m^2 g^{-1} C)	0.26±0.12	0.19±0.08	0.23±0.11	0.19±0.06	0.33±0.11
FI	1.8±0.20	1.5±0.20	1.8±0.23	2.0±0.10	1.8±0.06
BIX	1.2±0.18	1.4±0.20	1.2±0.19	1.3±0.09	1.3±0.14
HIX	2.0±0.59	1.3±0.41	2.1±0.68	1.9±0.17	2.1±0.42
[a]Levoglucosan (ng C m^{-3})	222±485	362±438	185±654	42±16	280±185
[a]Levoglucosan/TSP (× 10^{-3})	2.9±2.9	3.4±3.1	2.3±3.6	1.9±0.98	3.9±1.8

277 a: described elsewhere (Wang et al., 2020a).

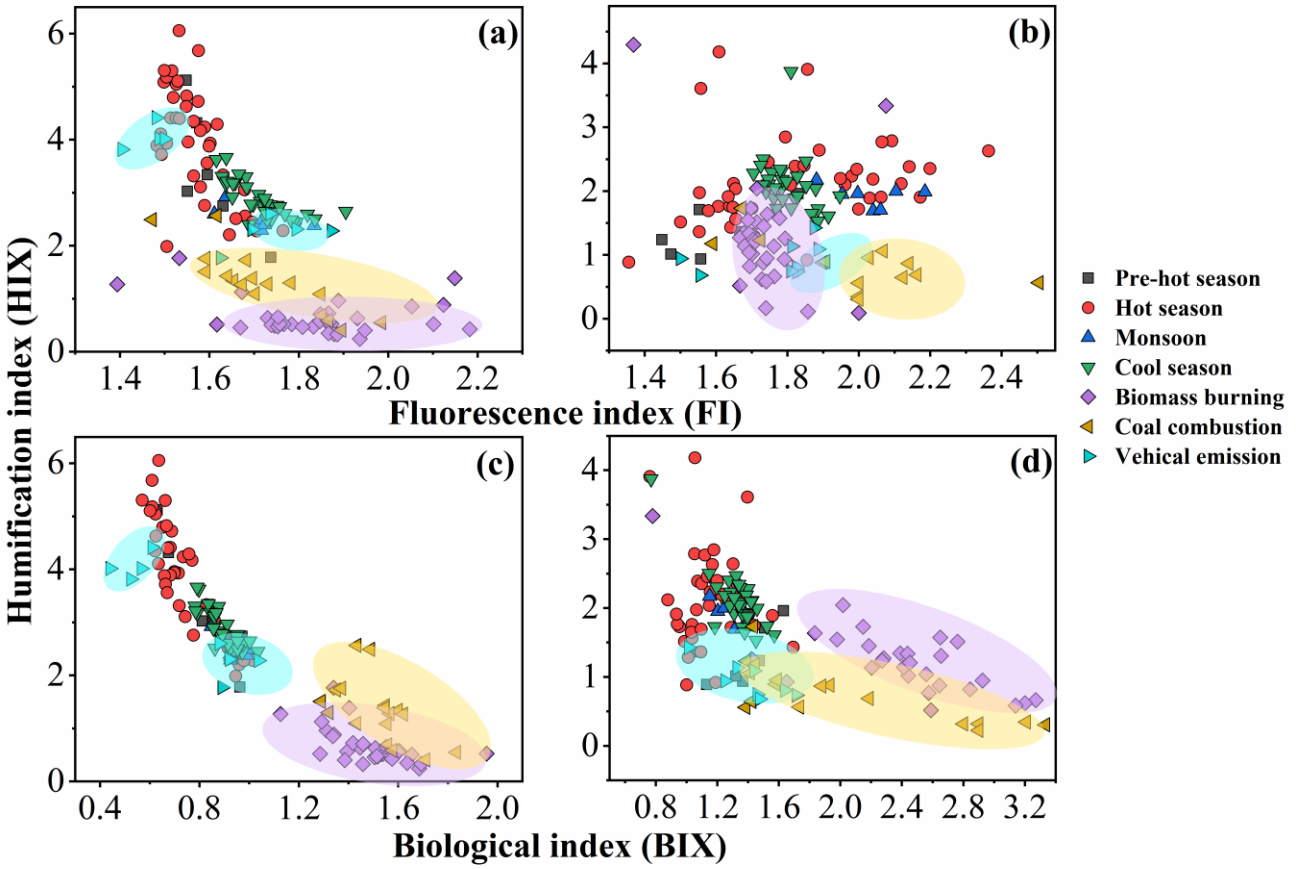

Figure 2. Fluorescence index (FI), biological index (BIX), and humification index (HIX) of water-soluble organic carbon (WSOC, a, c) and methanol-soluble organic carbon (MSOC, b, d) in aerosol samples from Bangkok, Thailand, as well as source emission samples including biomass burning, coal combustion and vehicle emission which were encircled by a violet, yellow, and blue region, respectively. Note that the fluorescence characteristic of source samples was described elsewhere (Tang et al., 2020b), but the fluorescence indices was first reported in this study. Pre-hot season is from January 18 to February 29, 2016; hot season is from March 2 to May 31, 2016; monsoon is from June 2 to October 30, 2016; cool season is from November 1, 2016 to January 28, 2017.

The BIX and FI were previously proposed as proxies for the contribution of biogenic organic matter and autochthonous biological activity in natural water, respectively (Fu et al., 2015;Qin et al., 2018). For example, the FI decreased by up to 20% indicating that the samples appeared increasingly like "terrestrial" DOM, whereas the BIX increased by up to 37% indicating that the samples became more "autochthonous" in character (Murphy et al., 2018;Gabor et al., 2014). FI values ≤ 1.4 correspond to terrestrially derived organics and higher aromaticity, whereas values ≥ 1.9 correspond to microbial sources and a lower aromatic carbon content (Mcknight et al., 2001). An increase in BIX is related to an increase in the contribution of microbially derived organics, with high values (> 1) shown to correspond to a predominantly biological or microbial origin of DOM and the presence of organic matter freshly released into water, whereas values ≤ 0.6 indicate the presence of little biological material (Huguet et al., 2009).

The FI and BIX values of the Bangkok aerosol samples are summarized in Table 1 and Fig. 2. The FI values of the WSOC and MSOC were 1.6±0.10 and 1.8±0.20, respectively, suggesting that these chromophores are representative of both terrestrially and microbially derived organic matter. The BIX values of the WSOC and MSOC were 0.82±0.13 and 1.2±0.18, respectively. Almost all BIX values were greater than 0.6 in the two fractions, suggesting biological or microbial contribution. Lee et al. (2013) reported that the BIX values of SOA samples averaged 0.6 and increased upon aging. In addition, the results of our source samples showed that primary biomass-burning and coal-combustion samples had high FI and BIX values (Fig. 2). These results indicate that these chromophores in Bangkok were likely freshly introduced or derived from biomass burning and coal combustion. Further, an increase in BIX in the MSOC in comparison with the WSOC was observed in primary biomass-burning and coal-combustion samples, consistent with the Bangkok samples. The BIX values were similar to those in the WSOC in Arctic aerosols (0.6–0.96, mean: 0.72), which were within the extreme values for the predominance of humic- or protein-like fluorophores (Fu et al., 2015). BIX values exhibited the opposite trend from HIX values, with low BIX values in the hot season. This may be explained by a previous study showing that a high BIX appears to indicate little humification (Birdwell and Engel, 2010). It should be noted that the fluorescence indices (FI, BIX, and HIX) were first applied for aquatic and soil organic compounds and further extended to the atmosphere due to the similarities in the properties of organic matter (Graber and Rudich, 2006). However, the values observed for primary biomass burning and coal combustion in this study differ from with the previously established fluorescence standards for aquatic environments and soil. Therefore, caution is required when using these indices to appoint source of atmospheric chromophores (Wu et al., 2021).

3.3. Optical properties of dissolved BrC.

Figure 3 shows the variations in soluble OC concentrations and the corresponding light absorption coefficient at 365 nm (Abs_{365}). In general, the Abs_{365} closely tracked the variations in the mass concentrations of WSOC and MSOC ($p < 0.000$, $R^2 = 0.95$ and $p < 0.000$, $R^2 = 0.75$, respectively) (Fig. S11), indicating that the portions of BrC in both fractions were considerably stable. Furthermore, light absorption at 365nm were higher in the pre-hot season, hot season, and cool season than that in the monsoon season. According to the levoglucosan level that generally regarded as biomass burning tracers and the ratios of levoglucosan/TSP (Table 1), we infer that the non-monsoon season were more affected by biomass burning and also showed high absorption.

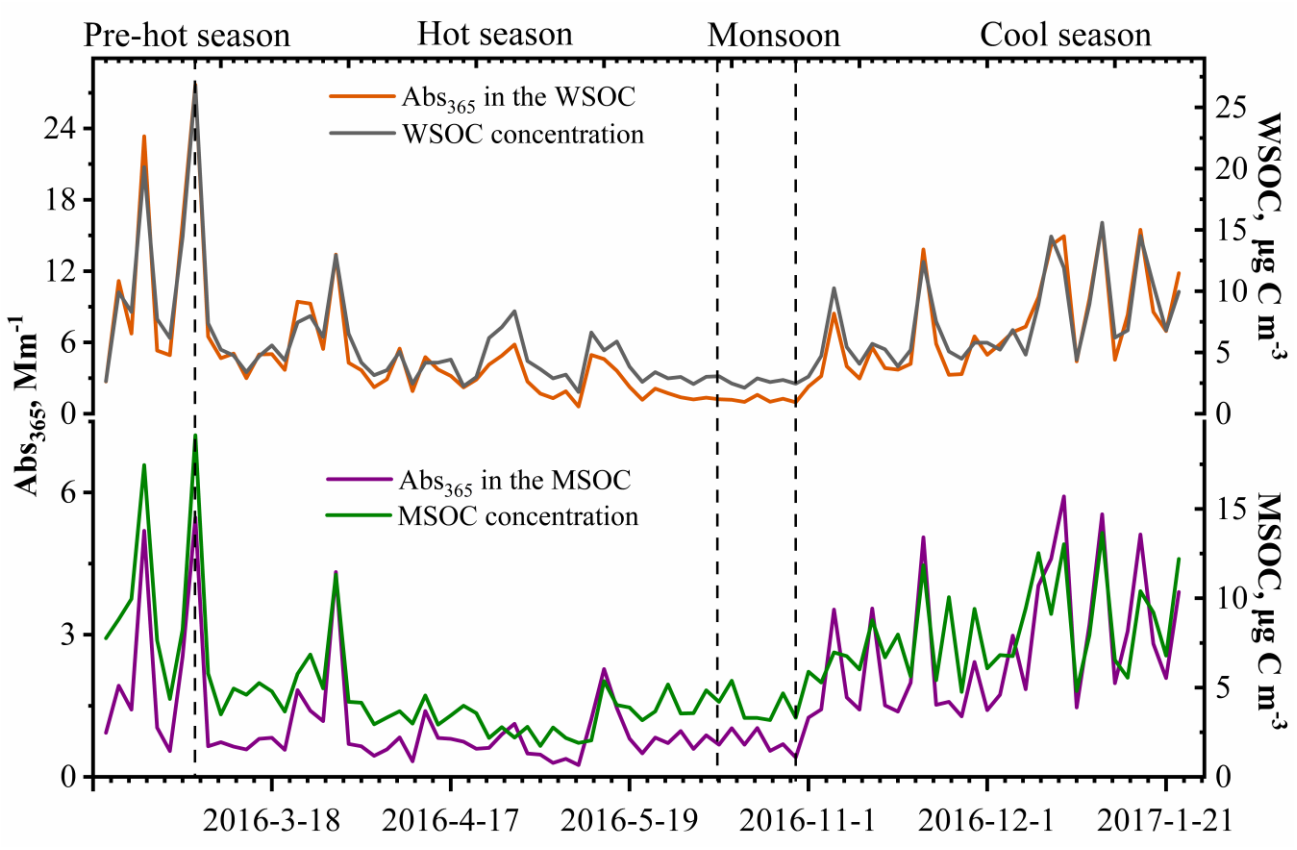

Figure 3. Time series plots of water-soluble organic carbon (WSOC) and methanol-soluble organic carbon (MSOC) concentration (μg C m^{-3}) and water- and methanol-extract light absorption coefficient at 365 nm (Abs_{365}) (Mm^{-1}) in the aerosol samples from Bangkok, Thailand during 2016–2017.

The absorption Ångström exponent (AAE) and mass absorption efficiency (MAE) are important optical parameters reflecting the spectral dependence and light absorption ability of BrC, respectively. The magnitude of the AAE reflects the differences in BrC source and atmospheric processes (Lack et al., 2013). Typically, the AAE value is close to 1 when light absorption is dominated by soot (Kirchstetter et al., 2004), roughly 1–3 for simulated biomass-burning aerosols (Hopkins et al., 2007), and up to 6–7 for water-soluble HULIS in biomass burning-impacted aerosols (Hoffer et al., 2006). The AAE values of the WSOC and MSOC between 330 and 400 nm in this study were up to 5.1±0.68 and 5.2±0.94 (Fig. 4), respectively, indicating strong wavelength dependence in the light absorption capability. These high values show that BrC tends to absorb more solar irradiation over ultraviolet wavelengths, which is comparable to BC absorption as shown in Fig. S12. These observations indicate that BrC has important impacts on photochemical reactions in the atmosphere (Barnard et al., 2008). The AAE values in this study are similar to those of water-soluble BrC over biomass burning-impacted regions, such as Beijing (Mo et al., 2018;Yan et al., 2015) and Guangzhou (Liu et al., 2018), but lower than those of aerosols from simulated biomass-burning and coal-combustion experiments (Fan et al., 2018;Tang et al., 2020a;Li et al., 2018). However, it should be noted that the BrC AAE varies in the

atmosphere. Dasari et al. (2019) reported that AAE values of water-soluble BrC increase continuously due to photolysis of chromophores and atmospheric oxidation during long-range transport over the Indo-Gangetic Plain (IGP). In addition, pH changes can cause the absorption spectra of some BrC species to shift to longer wavelengths upon deprotonation, decreasing AAE values (Mo et al., 2017). The pH values of WSOC fraction for all the samples were within the range of 5–7, generally thinking it didn't affect the absorbance according to a prior study (Chen et al., 2016a).

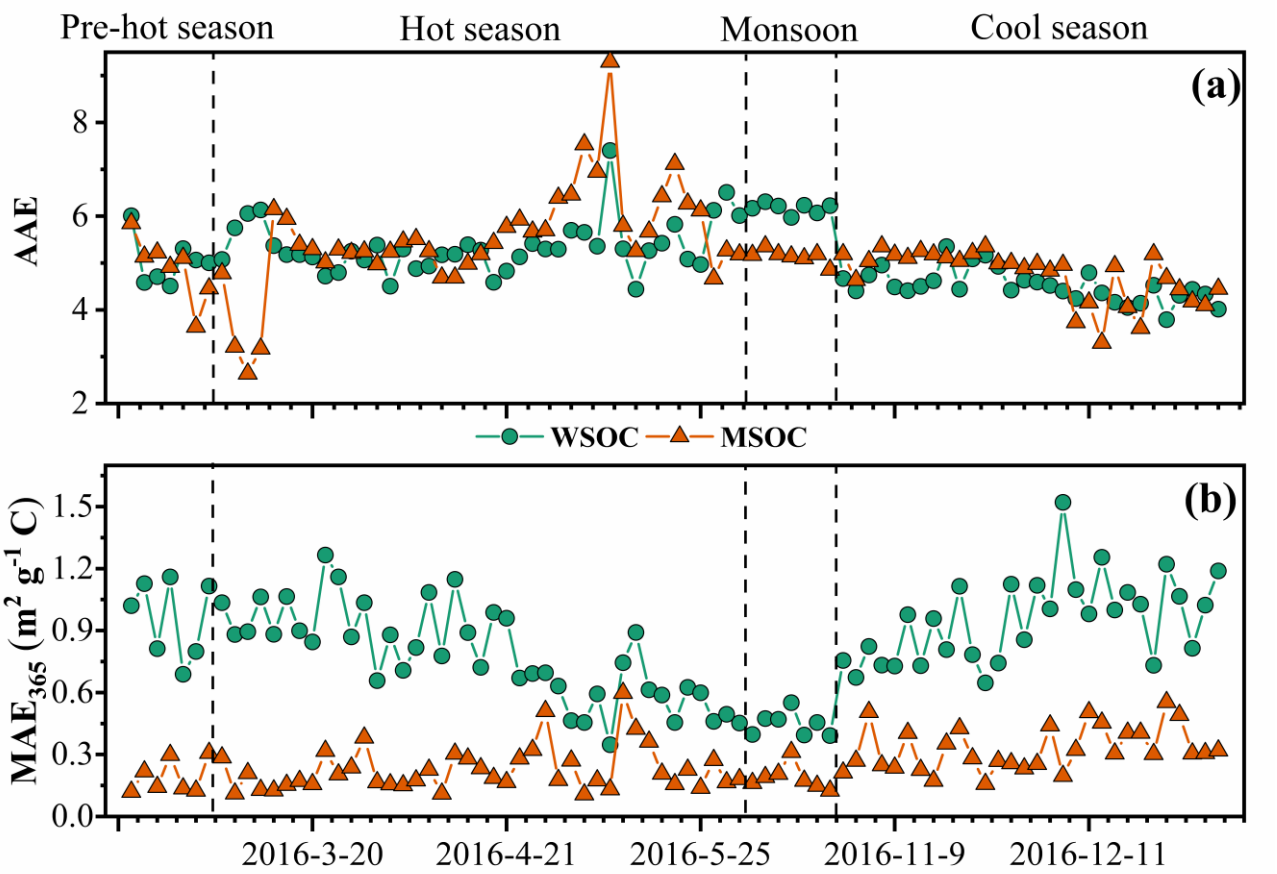

Figure 4. Time series plots of Absorption Ångström exponent (AAE, a), the mass absorption efficiency at 365 nm (MAE_{365}, b) in the water-soluble organic carbon (WSOC) and methanol-soluble organic carbon (MSOC) in aerosols samples from Bangkok in Thailand during 2016–2017.

The MAE at 365 nm (MAE_{365}) of the WSOC was 0.83±0.25 m^2 g^{-1} C, which was higher than that of the MSOC (0.26±0.12 m^2 g^{-1} C), indicating that more water-soluble BrC with stronger light absorption capability could be extracted with ultrapure deionized water, whereas water-insoluble BrC is characterized by lower light absorption capability over Bangkok. These results were consistent with those from vehicular exhaust samples in our previous study, where MAE_{365} values of the WSOC (0.71±0.30 m^2 g^{-1} C) were higher than those of the MSOC (0.26±0.09 m^2 g^{-1} C) (Tang et al., 2020b). Opposite results have been shown for primary biomass burning and coal combustion (Tang et al., 2020b). Similarly, Bikkina et al. (2020) observed that the marine-impacted aerosols of the Bay of

Bengal showed higher MAE_{365} values in the WSOC fraction than MSOC fraction (only extract using methanol), and they explained it due to two plausible reasons. First, the BrC aerosols over Bay of Bengal have a contribution from a different source (i.e., maritime influence) and contain BrC-chromophores that are more soluble in water than methanol. Secondary, there could be significant photobleaching effects of different chromophores. However, Wu et al. (2020b) reported that the MAE_{365} values of ~~MSOC~~ methanol-extracts are higher than those of WSOC in ~~summer~~winter, whereas the situation is reversed in ~~winter~~summer. Therefore, we infer that the different sources and atmospheric processes would impact the distribution of water-soluble and methanol-soluble chromophores. Considering the high temperature and humidity (Table S1), and tropical monsoon climate in Thailand, it seems to promote more water-soluble chromophores over Thailand. As not all water-insoluble components can be extracted with methanol, the observed light absorption by MSOC would therefore likely reflect the lower limit. Table S3 shows a comparison of the MAE values of Bangkok aerosols with those of other regions, indicating a medium light absorption capacity. The MAE_{365} values of the water-soluble fraction in this study were comparable to those of Nanjing (Chen et al., 2018), Guangzhou (Liu et al., 2018), and Beijing in summer (Yan et al., 2015), but lower than those of $PM_{2.5}$ from Singapore (Adam et al., 2020), PM_{10} from Godavari, Nepal, in the pre-monsoon season (Wu et al., 2019), and smoke particles from biomass burning and coal combustion (Park and Yu, 2016;Fan et al., 2018;Tang et al., 2020b). Lower MAE_{365} values of both fractions were observed in the monsoon season than in the non-monsoon seasons, likely due to the heavy monsoon rains that effectively remove soluble gases and aerosols (Lawrence and Lelieveld, 2010) and/or reduce biomass-burning activity (levoglucosan level in Table 1). A previous study reported similar findings in the USA in that the MAE_{365} was approximately three-fold higher in biomass burning-impacted samples than in non-biomass burning-impacted samples (Hecobian et al., 2010). Another study in the central Tibetan Plateau highlighted that BrC emitted by biomass burning has stronger light absorption capability than does secondary BrC formed in the atmosphere (Wu et al., 2018). On the Indo-China peninsula, Bangkok receives 99% of the fire-derived aerosols from December to April (Lee et al., 2017), which may explain the high absorption levels in the non-monsoon seasons.

3.4. Chromophores responsible for BrC light absorption.

EEM analysis enables the probing of the chemical structure of DOM because of its ability to distinguish among different classes of organic matter (Wu et al., 2003). Generally, BrC absorption is related to the chromophores within it and is susceptible to change with variations in chemical properties, e.g., oxidation level (Mo et al., 2018), degree of unsaturation (Jiang et al., 2020), molecular weight (Tang et al., 2020b;Di Lorenzo et al., 2017), functional groups (Chen et al., 2017b), molecular

composition, etc (Song et al., 2019;Lin et al., 2018). The fluorescence intensity of each EEM component was shown to be associated with light absorption indices, such as MAE_{365} and AAE, of HULIS in controlled crop straw-combustion experiments (Huo et al., 2018). As a linear relationship between organic matter concentration and fluorescence intensity can be assumed for very dilute samples due to the IFE (Murphy et al., 2013), we have corrected our fluorescence data for IFE using absorbance to enable "clean " correlation analysis (as shown in Fig. S13 a, b). The linear regression slopes in the scatter plots of Abs_{365} versus WSOC or MSOC could mathematically represent the average MAE values of WSOC or MSOC at 365 nm, respectively (Fig. S11 a, b). The phenomenon indicates that both fluorescence and Abs_{365} data point to similar relationships between sources or chemical processes with organic matter concentrations, and therefore, we attempted to link the fluorescence results to BrC absorption. It should be noted that light-absorbing substances in atmospheric particulate matter are not necessarily all fluorescent, such as nitrophenol compounds, which are a type of BrC commonly found in the atmospheric particulate matter; however, there is no strong fluorescence signal with which to scan the nitrophenol standards (Chen et al., 2019a).

In order to evaluate the light absorption from different fluorescent chromophores, ~~W~~we used MLR to explore the relationship between the fluorescence intensities of chromophores and Abs_{365}. In this study, light absorption properties were treated as the dependent variables, and the fluorescence were independent variables. During MLR, insignificant fluorescent components were excluded from the regression using a stepwise screening process to avoid overfitting ($F_{inclusion}$: $p < 0.05$; $F_{elimination}$: $p > 0.10$). The MLR statistical metrics are listed in Tables S4 and S5. For the independent variables with significant correlations with the dependent variable ($p < 0.05$), or with positive contributions to the independence, Abs_{365}, they will be retained in the statistical model as the efficiency factors to Abs_{365}. Thus, ~~F~~for the WSOC fraction, a revised model (regression 3) equation was used with an adjusted R^2 of 0.995. The final optimized equations were $Abs_{365} = 0.765 \times P4 + 0.051 \times P2 + 0.091 \times P7$, for the WSOC fraction, and $Abs_{365} = 0.238 \times C4$ for the MSOC fraction (Table S5). The model errors for water-soluble and methanol-soluble Abs_{365} were −5.5%–64% and −34%–58%, respectively. The predicted Abs_{365} values fit the measured values well (Fig. 5, slope = 0.99 and 0.95, and $R^2 = 0.99$ and 0.94 for WSOC and MSOC, respectively).

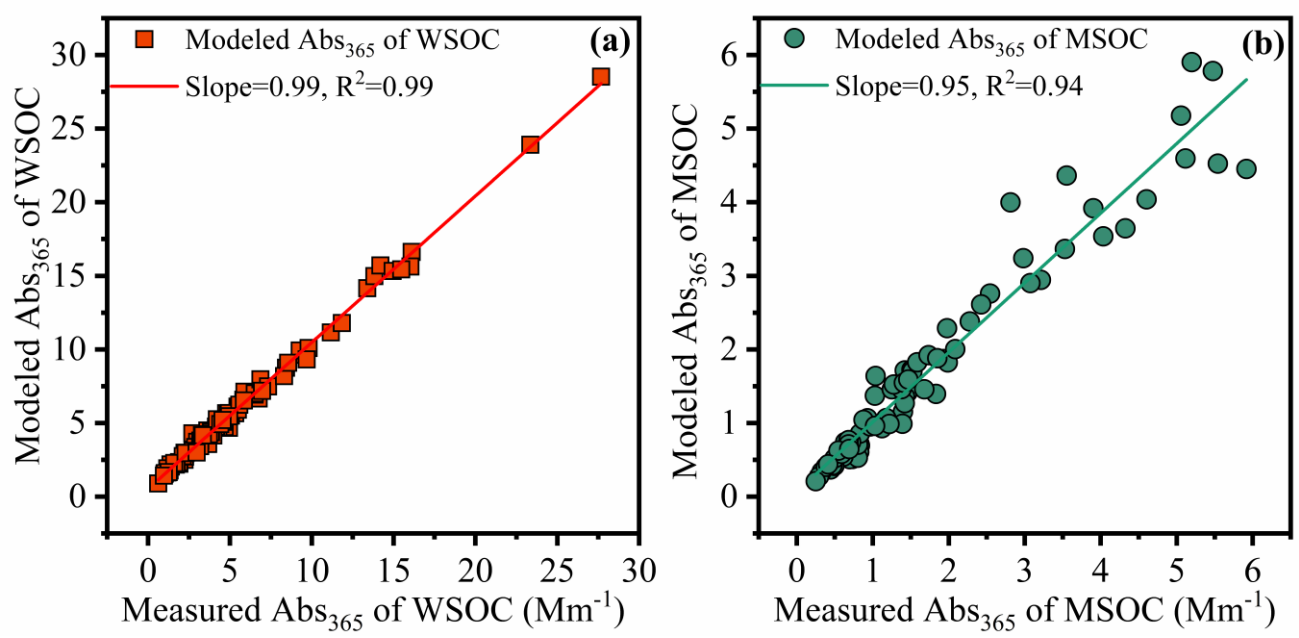

Figure 5. Linear correlation analysis between modeling Abs_{365} using multiple linear regression (MLR) analysis and measured Abs_{365} in the water-soluble organic carbon (WSOC, a) and methanol-soluble organic carbon (MSOC, b) in aerosols samples from Bangkok in Thailand during 2016–2017, respectively. Note that the fluorescent intensities of parallel factor (PARAFAC) model results (fluorescent components) were used as variables in MLR analysis.

For water-soluble BrC, the P4 component had the largest coefficient with Abs_{365}, which was much higher than those for P2 and P7. The C4 component had the largest coefficient with Abs_{365} for methanol-soluble BrC. These results indicate that the light absorption by BrC is more dependent on chromophores with longer emission wavelengths (P4 and C4). These characteristics also indicate that the strongly absorbing substances in BrC probably originate from large conjugated electron functional groups or include donor and acceptor molecules for charge-transfer interactions (Del Vecchio and Blough, 2004;Cory and McKnight, 2005). Kellerman et al. (2015) reported that these components are highly aromatic and oxygen-rich with high apparent molecular weight. These important findings highlight that larger chromophores may be the most persistent BrC species in the atmosphere and hence exert the greatest influence for perturbing the global radiative balance.

To further interpret the BrC source profiles as real-world TSP sources, we examined 84 (minus one missing value) TSP samples from Bangkok using the US EPA PMF5.0 model. All samples were merged together to form an 84 × 30 dataset (84 samples with 30 species). The initial data of positive matrix factorization input were from our previous study (Wang et al., 2020a). We further added Abs_{365} values of WSOC and MSOC, and the fluorescence intensities (in RU) of P2, P4, P7, and C4 components to the model. A seven-factor solution was achieved that provided the most physically reasonable source profiles (Fig. S14), including ship emission, secondary sulfate, dust, land fossil-fuel combustion, sea salt, biomass burning, and industrial emission, consistent with our previous study

(Wang et al., 2020a). Figure ~~S14~~ S15 ~~also~~ shows the contributions of the above sources to light absorption at λ= 365 nm, which represent the fraction of BrC for each factor. Biomass burning was found to be the main source of BrC over Bangkok; ~~61~~58% and ~~67~~74% for water-soluble and methanol-soluble BrC, respectively. These were comparable to previous observations using a similar approach in Xi'an (55%) (Wu et al., 2020a). The time-series of Abs_{365} of WSOC and MSOC contributed by factors shows the high biomass burning contribution is related to the higher local fire spots (i.e., pre-hot season, hot season, and cool season) and/or air mass from the continent (Fig. S16–S17). Jiang et al. (2021) observed increases in biomass burning contributions to BrC absorption during the winter period that was dominant in continental-origin air masses. Furthermore, the P4 and C4 components, which were more closely associated with Abs_{365}, could be mostly attributed to biomass burning (~~64~~54% and ~~66~~70%, respectively) as shown in Fig. 6. Our previous study showed that biomass burning accounted for a considerably large portion (mean: 26%) of the TSP mass concentration in the same samples (Wang et al., 2020a). This result suggests that biomass burning makes a significant contribution to not only particulate matter but also BrC light absorption.

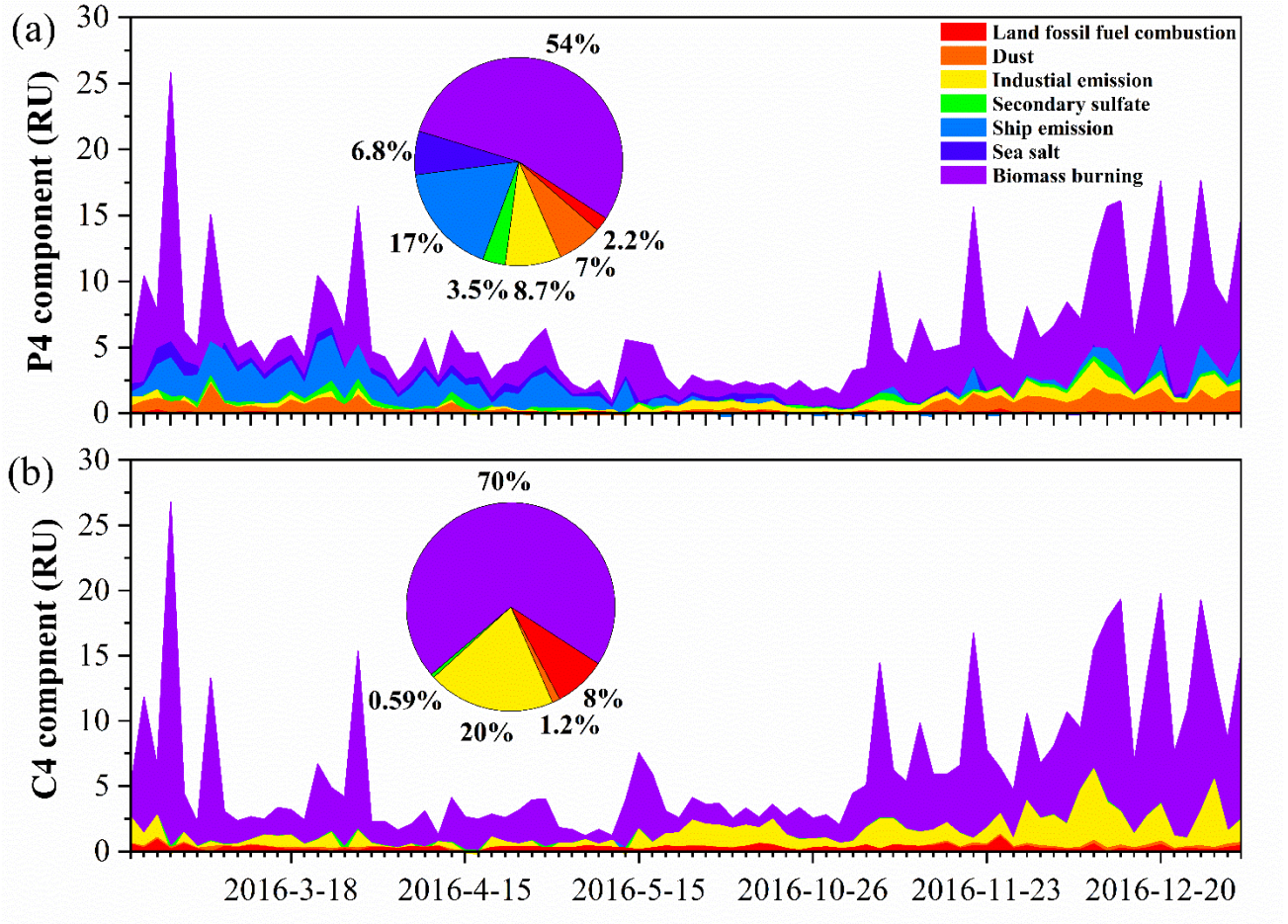

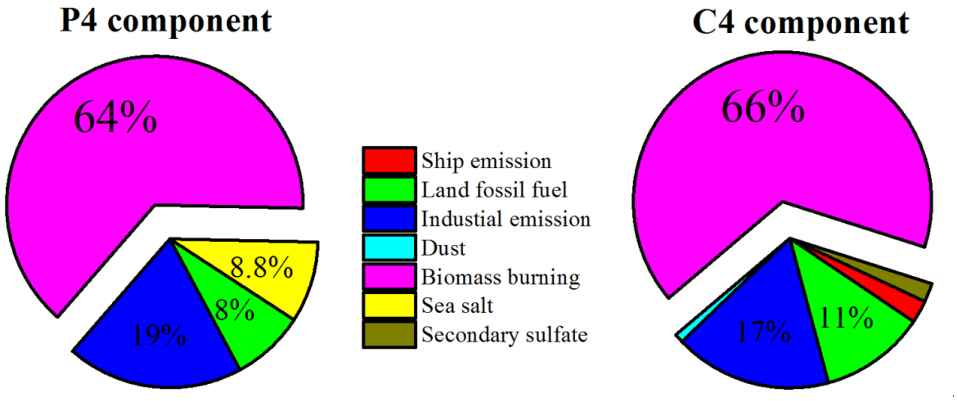

Figure 6. The time-series of P4 component of the WSOC (a) and C4 of the MSOC (b) in TSP samples over Bangkok in Thailand contributed by each factor resolved by ~~P~~positive matrix ~~factorization~~ factorization~~derived source apportionment of chromophores P4 of the WSOC and C4 of the MSOC in TSP samples over Bangkok in Thailand during 2016–2017~~.

4. Conclusions

This study presents a comprehensive analysis of water- and methanol-soluble chromophores in aerosol samples over Bangkok in Thailand during 2016–2017. EEM combining with PARAFAC analysis showed that the identified fluorescent components were humic-like and protein-like

substances but different patterns in the WSOC and MSOC, indicating different chemical compositions. By adding three-source fluorescence into the original PARAFAC model, we found that chromophores with longer emission wavelengths in the atmosphere may be due to atmospheric chemical reactions or "aging" by both bleaching the source chromophores or producing new chromophores. We also suggest that caution is required when using fluorescence indices to appoint source of atmospheric chromophores. In addition, more water-soluble BrC with stronger light absorption capability could be extracted with ultrapure deionized water over Bangkok (0.83±0.25 vs. 0.26±0.12 m^2 g^{-1} C), and both water-soluble and methanol-soluble BrC exhibited a high light-absorption in non-monsoon seasons due to the influence of biomass burning. The MLR analysis showed that both the light absorption of BrC at 365 nm in the two fractions was significantly dependent on the special fluorescent chromophores with longer emission wavelength that are generally highly aromatic and oxygen-rich with high apparent molecular weight. Positive matrix factorization model results further showed that biomass burning was main contributor of these fluorescent chromophores (up to ~~60~~50%). In summary, this study provides a new insight into BrC absorption and sources, which may promote the application of EEM spectroscopy to predict and model the light absorption of BrC in the atmosphere.

Data availability. The data used in this study are available upon request. Please contact Guangcai Zhong (gczhong@gig.ac.cn).

Supplement. The supplement related to this article is available.

Author contributions. JT, GZ, JL, and GZ (Guangcai Zhong) designed the experiment. JT and JW carried out the measurements and analyzed the data. JW and SB organized and performed the samplings. JT (Jianhui Tang) supported the fluorescence instruments and laboratory. CT and HJ supported the models. JT wrote the paper. JL, GZ (Guangcai Zhong), YC, YM, BZ, XG, and GZ reviewed and commented on the paper.

Competing interests. The authors declare that they have no conflict of interest.

Acknowledgements: This research has been supported by the National Natural Science Foundation of China (42030715, 41430645 and 41773120), the International Partnership Program of Chinese Academy of Sciences (grant no. 132744KYSB20170002), Guangdong Foundation for Program of Science and Technology Research (Grant Nos. 2017BT01Z134, 2018A030310022, ~~2017B030314057 and~~ 2019B121205006, and 2020B1212060053), and China Postdoctoral Science Foundation (2020M682937).

References

Adam, M. G., Chiang, A. W. J., and Balasubramanian, R.: Insights into characteristics of light absorbing

carbonaceous aerosols over an urban location in Southeast Asia, Environ. Pollut., 257, 113425, https://doi.org/10.1016/j.envpol.2019.113425, 2020.

Alexander, D. T. L., Crozier, P. A., and Anderson, J. R.: Brown carbon spheres in East Asian outflow and their optical properties, Science, 321, 833-836, https://doi.org/10.1126/science.1155296, 2008.

Andersson, C. A., and Bro, R.: The N-way Toolbox for MATLAB, Chemom. Intell. Lab. Syst., 52, 1-4, https://doi.org/10.1016/s0169-7439(00)00071-x, 2000.

Babar, Z. B., Park, J.-H., and Lim, H.-J.: Influence of NH 3 on secondary organic aerosols from the ozonolysis and photooxidation of α-pinene in a flow reactor, Atmos. Environ., 164, 71-84, https://doi.org/10.1016/j.atmosenv.2017.05.034, 2017.

Bahram, M., Bro, R., Stedmon, C., and Afkhami, A.: Handling of Rayleigh and Raman scatter for PARAFAC modeling of fluorescence data using interpolation, J. Chemom., 20, 99-105, https://doi.org/10.1002/cem.978, 2006.

Barnard, J. C., Volkamer, R., and Kassianov, E. I.: Estimation of the mass absorption cross section of the organic carbon component of aerosols in the Mexico City Metropolitan Area, Atmos. Chem. Phys., 8, 6665-6679, http://doi.org/10.5194/acp-8-6665-2008, 2008.

Bianco, A., Minella, M., De Laurentiis, E., Maurino, V., Minero, C., and Vione, D.: Photochemical generation of photoactive compounds with fulvic-like and humic-like fluorescence in aqueous solution, Chemosphere, 111, 529-536, https://doi.org/10.1016/j.chemosphere.2014.04.035, 2014.

Bianco, A., Passananti, M., Deguillaume, L., Mailhot, G., and Brigante, M.: Tryptophan and tryptophan-like substances in cloud water: Occurrence and photochemical fate, Atmos. Environ., 137, 53-61, https://doi.org/10.1016/j.atmosenv.2016.04.034, 2016.

Bikkina, P., Bikkina, S., Kawamura, K., Sudheer, A. K., Mahesh, G., and Kumar, S. K.: Evidence for brown carbon absorption over the Bay of Bengal during the southwest monsoon season: a possible oceanic source, Environ Sci Process Impacts, 22, 1743-1758, https://doi.org/10.1039/d0em00111b, 2020.

Birdwell, J. E., and Engel, A. S.: Characterization of dissolved organic matter in cave and spring waters using UV–Vis absorbance and fluorescence spectroscopy, Org. Geochem., 41, 270-280, https://doi.org/10.1016/j.orggeochem.2009.11.002, 2010.

Birdwell, J. E., and Valsaraj, K. T.: Characterization of dissolved organic matter in fogwater by excitation–emission matrix fluorescence spectroscopy, Atmos. Environ., 44, 3246-3253, https://doi.org/10.1016/j.atmosenv.2010.05.055, 2010.

Chen, H., Liao, Z. L., Gu, X. Y., Xie, J. Q., Li, H. Z., and Zhang, J.: Anthropogenic Influences of Paved Runoff and Sanitary Sewage on the Dissolved Organic Matter Quality of Wet Weather Overflows: An Excitation-Emission Matrix Parallel Factor Analysis Assessment, Environ. Sci. Technol., 51, 1157-1167, https://doi.org/10.1021/acs.est.6b03727, 2017a.

Chen, Q., Ikemori, F., and Mochida, M.: Light Absorption and Excitation-Emission Fluorescence of Urban Organic Aerosol Components and Their Relationship to Chemical Structure, Environ. Sci. Technol., 50, 10859-10868, https://doi.org/10.1021/acs.est.6b02541, 2016a.

Chen, Q., Miyazaki, Y., Kawamura, K., Matsumoto, K., Coburn, S., Volkamer, R., Iwamoto, Y., Kagami, S., Deng,

542 Y., Ogawa, S., Ramasamy, S., Kato, S., Ida, A., Kajii, Y., and Mochida, M.: Characterization of Chromophoric
543 Water-Soluble Organic Matter in Urban, Forest, and Marine Aerosols by HR-ToF-AMS Analysis and Excitation-
544 Emission Matrix Spectroscopy, Environ. Sci. Technol., 50, 10351-10360,
545 https://doi.org/10.1021/acs.est.6b01643, 2016b.
546 Chen, Q., Ikemori, F., Nakamura, Y., Vodicka, P., Kawamura, K., and Mochida, M.: Structural and Light-Absorption
547 Characteristics of Complex Water-Insoluble Organic Mixtures in Urban Submicrometer Aerosols, Environ. Sci.
548 Technol., 51, 8293-8303, https://doi.org/10.1021/acs.est.7b01630., 2017b.
549 Chen, Q., Mu, Z., Song, W., Wang, Y., Yang, Z., Zhang, L., and Zhang, Y. L.: Size - Resolved Characterization of
550 the Chromophores in Atmospheric Particulate Matter From a Typical Coal-Burning City in China, J. Geophys.
551 Res.-Atmos., 124, 10546-10563, https://doi.org/10.1029/2019jd031149, 2019a.
552 Chen, Q., Wang, M., Wang, Y., Zhang, L., Li, Y., and Han, Y.: Oxidative Potential of Water-Soluble Matter Associated
553 with Chromophoric Substances in PM2.5 over Xi'an, China, Environ. Sci. Technol., 53, 8574-8584,
554 https://doi.org/10.1021/acs.est.9b01976, 2019b.
555 Chen, W., Westerhoff, P., Leenheer, J. A., and Booksh, K.: Fluorescence excitation - Emission matrix regional
556 integration to quantify spectra for dissolved organic matter, Environ. Sci. Technol., 37, 5701-5710,
557 https://doi.org/10.1021/es034354c 2003.
558 Chen, Y., and Bond, T. C.: Light absorption by organic carbon from wood combustion, Atmos. Chem. Phys., 10,
559 1773-1787, https://doi.org/10.5194/acp-10-1773-2010, 2010.
560 Chen, Y., Ge, X., Chen, H., Xie, X., Chen, Y., Wang, J., Ye, Z., Bao, M., Zhang, Y., and Chen, M.: Seasonal light
561 absorption properties of water-soluble brown carbon in atmospheric fine particles in Nanjing, China, Atmos.
562 Environ., 230-240, https://doi.org/10.1016/j.atmosenv.2018.06.002, 2018.
563 Cory, R. M., and McKnight, D. M.: Fluorescence spectroscopy reveals ubiquitous presence of oxidized and reduced
564 quinones in dissolved organic matter, Environ. Sci. Technol., 39, 8142-8149, https://doi.org/10.1021/es0506962,
565 2005.
566 Dasari, S., Andersson, A., Bikkina, S., Holmstrand, H., Budhavant, K., Satheesh, S., Asmi, E., Kesti, J., Backman, J.,
567 Salam, A., Bisht, D. S., Tiwari, S., Hameed, Z., and Gustafsson, O.: Photochemical degradation affects the light
568 absorption of water-soluble brown carbon in the South Asian outflow, Sci. Adv., 5, 10,
569 https://doi.org/10.1126/sciadv.aau8066, 2019.
570 Del Vecchio, R., and Blough, N. V.: On the Origin of the Optical Properties of Humic Substances, Environ. Sci.
571 Technol., 38, 3885-3891, https://doi.org/10.1021/es049912h, 2004.
572 Di Lorenzo, R. A., Washenfelder, R. A., Attwood, A. R., Guo, H., Xu, L., Ng, N. L., Weber, R. J., Baumann, K.,
573 Edgerton, E., and Young, C. J.: Molecular-Size-Separated Brown Carbon Absorption for Biomass-Burning
574 Aerosol at Multiple Field Sites, Environ. Sci. Technol., 51, 3128-3137, https://doi.org/10.1021/acs.est.6b06160,
575 2017.
576 Fan, X., Li, M., Cao, T., Cheng, C., Li, F., Xie, Y., Wei, S., Song, J., and Peng, P. a.: Optical properties and oxidative
577 potential of water- and alkaline-soluble brown carbon in smoke particles emitted from laboratory simulated
578 biomass burning, Atmos. Environ., 194, 48-57, https://10.1016/j.atmosenv.2018.09.025, 2018.
579 Fan, X. J., Cao, T., Yu, X. F., Wang, Y., Xiao, X., Li, F. Y., Xie, Y., Ji, W. C., Song, J. Z., and Peng, P. A.: The

evolutionary behavior of chromophoric brown carbon during ozone aging of fine particles from biomass burning, Atmos. Chem. Phys., 20, 4593-4605, https://10.5194/acp-20-4593-2020, 2020.

Fu, P., Kawamura, K., Chen, J., Qin, M., Ren, L., Sun, Y., Wang, Z., Barrie, L. A., Tachibana, E., Ding, A., and Yamashita, Y.: Fluorescent water-soluble organic aerosols in the High Arctic atmosphere, Sci Rep, 5, 9845, https://doi.org/10.1038/srep09845, 2015.

Fujii, Y., Iriana, W., Oda, M., Puriwigati, A., Tohno, S., Lestari, P., Mizohata, A., and Huboyo, H. S.: Characteristics of carbonaceous aerosols emitted from peatland fire in Riau, Sumatra, Indonesia, Atmos. Environ., 87, 164-169, https://doi.org/10.1016/j.atmosenv.2014.01.037, 2014.

Gabor, R. S., Baker, A., McKnight, D. M., and Miller, M. P.: Fluorescence Indices and Their Interpretation, in: Aquatic Organic Matter Fluorescence, edited by: Baker, A., Reynolds, D. M., Lead, J., Coble, P. G., and Spencer, R. G. M., Cambridge Environmental Chemistry Series, Cambridge University Press, Cambridge, 303-338, 2014.

Gao, Y., and Zhang, Y.: Formation and photochemical investigation of brown carbon by hydroxyacetone reactions with glycine and ammonium sulfate, RSC Advances, 8, 20719-20725, https://doi.org/10.1039/c8ra02019a, 2018.

Graber, E. R., and Rudich, Y.: Atmospheric HULIS: How humic-like are they? A comprehensive and critical review, Atmos. Chem. Phys., 6, 729-753, https://doi.org/10.5194/acp-6-729-2006, 2006.

Gu, Q., and Kenny, J. E.: Improvement of Inner Filter Effect Correction Based on Determination of Effective Geometric Parameters Using a Conventional Fluorimeter, Anal. Chem., 81, 420-426, https://doi.org/10.1021/ac801676j, 2009.

Han, H., Kim, G., Seo, H., Shin, K.-H., and Lee, D.-H.: Significant seasonal changes in optical properties of brown carbon in the midlatitude atmosphere, Atmos. Chem. Phys., 20, 2709-2718, https://doi.org/10.5194/acp-20-2709-2020, 2020.

Hawkes, J. A., Patriarca, C., Sjöberg, P. J. R., Tranvik, L. J., and Bergquist, J.: Extreme isomeric complexity of dissolved organic matter found across aquatic environments, Limnol. Oceanogr. Lett., 3, 21-30, https://doi.org/10.1002/lol2.10064, 2018.

Hecobian, A., Zhang, X., Zheng, M., Frank, N., Edgerton, E. S., and Weber, R. J.: Water-Soluble Organic Aerosol material and the light-absorption characteristics of aqueous extracts measured over the Southeastern United States, Atmos. Chem. Phys., 10, 5965-5977, https://doi.org/10.5194/acp-10-5965-2010, 2010.

Hoffer, A., Gelencsér, A., Guyon, P., Kiss, G., Schmid, O., Frank, G., Artaxo, P., and Andreae, M.: Optical properties of humic-like substances (HULIS) in biomass-burning aerosols, Atmos. Chem. Phys., 6, 3563-3570, https://doi.org/10.5194/acp-6-3563-2006, 2006.

Hopkins, R. J., Lewis, K., Desyaterik, Y., Wang, Z., Tivanski, A. V., Arnott, W. P., Laskin, A., and Gilles, M. K.: Correlations between optical, chemical and physical properties of biomass burn aerosols, Geophys. Res. Lett., 34, https://doi.org/10.1029/2007gl030502, 2007.

Huang, K., Fu, J. S., Hsu, N. C., Gao, Y., Dong, X., Tsay, S.-C., and Lam, Y. F.: Impact assessment of biomass burning on air quality in Southeast and East Asia during BASE-ASIA, Atmos. Environ., 78, 291-302, https://doi.org/10.1016/j.atmosenv.2012.03.048, 2013.

Huguet, A., Vacher, L., Relexans, S., Saubusse, S., Froidefond, J. M., and Parlanti, E.: Properties of fluorescent dissolved organic matter in the Gironde Estuary, Org. Geochem., 40, 706-719,

https://doi.org/10.1016/j.orggeochem.2009.03.002, 2009.

Huo, Y., Li, M., Jiang, M., and Qi, W.: Light absorption properties of HULIS in primary particulate matter produced by crop straw combustion under different moisture contents and stacking modes, Atmos. Environ., 191, 490-499, https://doi.org/10.1016/j.atmosenv.2018.08.038, 2018.

Ishii, S. K., and Boyer, T. H.: Behavior of reoccurring PARAFAC components in fluorescent dissolved organic matter in natural and engineered systems: a critical review, Environ. Sci. Technol., 46, 2006-2017, https://doi.org/10.1021/es2043504, 2012.

Jiang, H., Li, J., Chen, D., Tang, J., Cheng, Z., Mo, Y., Su, T., Tian, C., Jiang, B., Liao, Y., and Zhang, G.: Biomass burning organic aerosols significantly influence the light absorption properties of polarity-dependent organic compounds in the Pearl River Delta Region, China, Environ. Int., 144, 106079, https://doi.org/10.1016/j.envint.2020.106079, 2020.

Jiang, H., Li, J., Sun, R., Liu, G., Tian, C., Tang, J., Cheng, Z., Zhu, S., Zhong, G., Ding, X., and Zhang, G.: Determining the Sources and Transport of Brown Carbon Using Radionuclide Tracers and Modeling, J. Geophys. Res.-Atmos., 126, https://doi.org/10.1029/2021jd034616, 2021.

Kasthuriarachchi, N. Y., Rivellini, L.-H., Chen, X., Li, Y. J., and Lee, A. K. Y.: Effect of relative humidity on secondary brown carbon formation in aqueous droplets, Environ. Sci. Technol., 54, 13207-13216, https://doi.org/10.1021/acs.est.0c01239, 2020.

Kellerman, A. M., Kothawala, D. N., Dittmar, T., and Tranvik, L. J.: Persistence of dissolved organic matter in lakes related to its molecular characteristics, Nat. Geosci., 8, 454-U452, https://doi.org/10.1038/ngeo2440, 2015.

Kirchstetter, T. W., Novakov, T., and Hobbs, P. V.: Evidence that the spectral dependence of light absorption by aerosols is affected by organic carbon, J. Geophys. Res.-Atmos., 109, https://doi.org/10.1029/2004jd004999, 2004.

Kirchstetter, T. W., and Thatcher, T. L.: Contribution of organic carbon to wood smoke particulate matter absorption of solar radiation, Atmos. Chem. Phys., 12, 5803-5816, https://doi.org/10.5194/acp-12-6067-2012, 2012.

Lack, D. A., Bahreini, R., Langridge, J. M., Gilman, J. B., and Middlebrook, A. M.: Brown carbon absorption linked to organic mass tracers in biomass burning particles, Atmos. Chem. Phys., 13, 2415-2422, https://doi.org/10.5194/acp-13-2415-2013, 2013.

Laskin, A., Laskin, J., and Nizkorodov, S. A.: Chemistry of atmospheric brown carbon, Chem. Rev., 115, 4335-4382, https://doi.org/10.1021/cr5006167, 2015.

Laskin, J., Laskin, A., and Nizkorodov, S. A.: Mass Spectrometry Analysis in Atmospheric Chemistry, Anal. Chem., 90, 166-189, https://doi.org/10.1021/acs.analchem.7b04249, 2018.

Lawrence, M. G., and Lelieveld, J.: Atmospheric pollutant outflow from southern Asia: a review, Atmos. Chem. Phys., 10, 11017-11096, https://doi.org/10.5194/acp-10-11017-2010, 2010.

Lee, H.-H., Bar-Or, R. Z., and Wang, C.: Biomass burning aerosols and the low-visibility events in Southeast Asia, Atmos. Chem. Phys., 17, 965-980, https://doi.org/10.5194/acp-17-965-2017, 2017.

Lee, H. J., Laskin, A., Laskin, J., and Nizkorodov, S. A.: Excitation-emission spectra and fluorescence quantum yields for fresh and aged biogenic secondary organic aerosols, Environ. Sci. Technol., 47, 5763-5770, https://doi.org/10.1021/es400644c, 2013.

Li, M., Fan, X., Zhu, M., Zou, C., Song, J., Wei, S., Jia, W., and Peng, P.: Abundances and light absorption properties of brown carbon emitted from residential coal combustion in China, Environ. Sci. Technol., 53, 595-603, https://doi.org/10.1021/acs.est.8b05630, 2018.

Lin, P., Laskin, J., Nizkorodov, S. A., and Laskin, A.: Revealing Brown Carbon Chromophores Produced in Reactions of Methylglyoxal with Ammonium Sulfate, Environ. Sci. Technol., 49, 14257-14266, https://doi.org/10.1021/acs.est.5b03608, 2015.

Lin, P., Aiona, P. K., Li, Y., Shiraiwa, M., Laskin, J., Nizkorodov, S. A., and Laskin, A.: Molecular Characterization of Brown Carbon in Biomass Burning Aerosol Particles, Environ. Sci. Technol., 50, 11815-11824, https://doi.org/10.1021/acs.est.6b03024, 2016.

Lin, P., Bluvshtein, N., Rudich, Y., Nizkorodov, S. A., Laskin, J., and Laskin, A.: Molecular Chemistry of Atmospheric Brown Carbon Inferred from a Nationwide Biomass Burning Event, Environ. Sci. Technol., 51, 11561-11570, https://doi.org/10.1021/acs.est.7b02276, 2017.

Lin, P., Fleming, L. T., Nizkorodov, S. A., Laskin, J., and Laskin, A.: Comprehensive Molecular Characterization of Atmospheric Brown Carbon by High Resolution Mass Spectrometry with Electrospray and Atmospheric Pressure Photoionization, Anal. Chem., 90, 12493-12502, https://doi.org/10.1021/acs.analchem.8b02177, 2018.

Liu, J., Bergin, M., Guo, H., King, L., Kotra, N., Edgerton, E., and Weber, R. J.: Size-resolved measurements of brown carbon in water and methanol extracts and estimates of their contribution to ambient fine-particle light absorption, Atmos. Chem. Phys., 13, 12389-12404, https://doi.org/10.5194/acp-13-12389-2013, 2013.

Liu, J., Mo, Y., Ding, P., Li, J., Shen, C., and Zhang, G.: Dual carbon isotopes ((14)C and (13)C) and optical properties of WSOC and HULIS-C during winter in Guangzhou, China, Sci. Total Environ., 633, 1571-1578, https://doi.org/10.1016/j.scitotenv.2018.03.293, 2018.

Luciani, X., Mounier, S., Redon, R., and Bois, A.: A simple correction method of inner filter effects affecting FEEM and its application to the PARAFAC decomposition, Chemom. Intell. Lab. Syst., 96, 227-238, https://doi.org/10.1016/j.chemolab.2009.02.008, 2009.

Marrero-Ortiz, W., Hu, M., Du, Z., Ji, Y., Wang, Y., Guo, S., Lin, Y., Gomez-Hermandez, M., Peng, J., Li, Y., Secrest, J., Levy Zamora, M., Wang, Y., An, T., and Zhang, R.: Formation and optical properties of brown carbon from small alpha-dicarbonyls and amines, Environ. Sci. Technol., https://doi.org/10.1021/acs.est.8b03995, 2018.

Matos, J. T. V., Freire, S. M. S. C., Duarte, R. M. B. O., and Duarte, A. C.: Natural organic matter in urban aerosols: Comparison between water and alkaline soluble components using excitation–emission matrix fluorescence spectroscopy and multiway data analysis, Atmos. Environ., 102, 1-10, https://doi.org/10.1016/j.atmosenv.2014.11.042, 2015.

Mcknight, D. M., Boyer, E. W., Westerhoff, P., Doran, P. T., Kulbe, T., and Andersen, D. T.: Spectrofluorometric characterization of dissolved organic matter for indication of precursor organic material and aromaticity, Limnol. Oceanogr., 46, 38-48, https://doi.org/10.4319/lo.2001.46.1.0038, 2001.

Mo, Y., Li, J., Jiang, B., Su, T., Geng, X., Liu, J., Jiang, H., Shen, C., Ding, P., Zhong, G., Cheng, Z., Liao, Y., Tian, C., Chen, Y., and Zhang, G.: Sources, compositions, and optical properties of humic-like substances in Beijing during the 2014 APEC summit: Results from dual carbon isotope and Fourier-transform ion cyclotron resonance mass spectrometry analyses, Environ. Pollut., 239, 322-331, https://doi.org/10.1016/j.envpol.2018.04.041, 2018.

694 Mo, Y. Z., Li, J., Liu, J. W., Zhong, G. C., Cheng, Z. N., Tian, C. G., Chen, Y. J., and Zhang, G.: The influence of
695 solvent and pH on determination of the light absorption properties of water-soluble brown carbon, Atmos.
696 Environ., 161, 90-98, https://doi.org/10.1016/j.atmosenv.2017.04.037, 2017.
697 Mounier, S., Patel, N., Quilici, L., Benaim, J. Y., and Benamou, C.: Fluorescence 3D de la matière organique dissoute
698 du fleuve amazone: (Three-dimensional fluorescence of the dissolved organic carbon in the Amazon river),
699 Water Res., 33, 1523-1533, https://doi.org/10.1016/S0043-1354(98)00347-9, 1999.
700 Murphy, K. R., Butler, K. D., Spencer, R. G., Stedmon, C. A., Boehme, J. R., and Aiken, G. R.: Measurement of
701 dissolved organic matter fluorescence in aquatic environments: an interlaboratory comparison, Environ. Sci.
702 Technol., 44, 9405-9412, https://doi.org/10.1021/es102362t, 2010.
703 Murphy, K. R., Stedmon, C. A., Graeber, D., and Bro, R.: Fluorescence spectroscopy and multi-way techniques.
704 PARAFAC, Anal. Methods, 5, 6557-6566, https://doi.org/10.1039/c3ay41160e, 2013.
705 Murphy, K. R., Timko, S. A., Gonsior, M., Powers, L. C., Wunsch, U. J., and Stedmon, C. A.: Photochemistry
706 Illuminates Ubiquitous Organic Matter Fluorescence Spectra, Environ. Sci. Technol., 52, 11243-11250,
707 https://doi.org/10.1021/acs.est.8b02648, 2018.
708 Park, S. S., and Yu, J.: Chemical and light absorption properties of humic-like substances from biomass burning
709 emissions under controlled combustion experiments, Atmos. Environ., 136, 114-122,
710 https://doi.org/10.1016/j.atmosenv.2016.04.022, 2016.
711 Permadi, D. A., Kim Oanh, N. T., and Vautard, R.: Assessment of emission scenarios for 2030 and impacts of black
712 carbon emission reduction measures on air quality and radiative forcing in Southeast Asia, Atmos. Chem. Phys.,
713 18, 3321-3334, https://doi.org/10.5194/acp-18-3321-2018, 2018.
714 Pohlker, C., Huffman, J. A., and Poschl, U.: Autofluorescence of atmospheric bioaerosols – fluorescent biomolecules
715 and potential interferences, Atmos. Meas. Tech., 5, 37-71, https://doi.org/10.5194/amt-5-37-2012, 2012.
716 Qin, J., Zhang, L., Zhou, X., Duan, J., Mu, S., Xiao, K., Hu, J., and Tan, J.: Fluorescence fingerprinting properties
717 for exploring water-soluble organic compounds in $PM_{2.5}$ in an industrial city of northwest China, Atmos.
718 Environ., 184, 203-211, https://doi.org/10.1016/j.atmosenv.2018.04.049, 2018.
719 Ramanathan, V., Li, F., Ramana, M. V., Praveen, P. S., Kim, D., Corrigan, C. E., Van Nguyen, H., Stone, E. A.,
720 Schauer, J. J., and Carmichael, G. R.: Atmospheric brown clouds: Hemispherical and regional variations in long-
721 range transport, absorption, and radiative forcing, J. Geophys. Res., 112, https://doi.org/10.1029/2006JD008124,
722 2007.
723 See, S. W., Balasubramanian, R., and Wang, W.: A study of the physical, chemical, and optical properties of ambient
724 aerosol particles in Southeast Asia during hazy and nonhazy days, J. Geophys. Res.-Atmos., 111,
725 https://doi.org/10.1029/2005JD006180, 2006.
726 Shimabuku, K. K., Kennedy, A. M., Mulhern, R. E., and Summers, R. S.: Evaluating Activated Carbon Adsorption
727 of Dissolved Organic Matter and Micropollutants Using Fluorescence Spectroscopy, Environ. Sci. Technol., 51,
728 2676-2684, https://doi.org/10.1021/acs.est.6b04911, 2017.
729 Song, J., Li, M., Jiang, B., Wei, S., Fan, X., and Peng, P.: Molecular Characterization of Water-Soluble Humic like
730 Substances in Smoke Particles Emitted from Combustion of Biomass Materials and Coal Using Ultrahigh-
731 Resolution Electrospray Ionization Fourier Transform Ion Cyclotron Resonance Mass Spectrometry, Environ.

Sci. Technol., 52, 2575-2585, https://doi.org/10.1021/acs.est.7b06126, 2018.

Song, J. Z., Li, M. J., Fan, X. J., Zou, C. L., Zhu, M. B., Jiang, B., Yu, Z. Q., Jia, W. L., Liao, Y. H., and Peng, P. A.: Molecular Characterization of Water- and Methanol-Soluble Organic Compounds Emitted from Residential Coal Combustion Using Ultrahigh-Resolution Electrospray Ionization Fourier Transform Ion Cyclotron Resonance Mass Spectrometry, Environ. Sci. Technol., 53, 13607-13617, https://doi.org/10.1021/acs.est.9b04331, 2019.

Stedmon, C. A., and Markager, S.: Resolving the variability in dissolved organic matter fluorescence in a temperate estuary and its catchment using PARAFAC analysis, Limnol. Oceanogr., 50, 686-697, https://doi.org/10.4319/lo.2005.50.2.0686, 2005.

Tang, J., Li, J., Mo, Y., Safaei Khorram, M., Chen, Y., Tang, J., Zhang, Y., Song, J., and Zhang, G.: Light absorption and emissions inventory of humic-like substances from simulated rainforest biomass burning in Southeast Asia, Environ. Pollut., 262, 114266, https://doi.org/10.1016/j.envpol.2020.114266, 2020a.

Tang, J., Li, J., Su, T., Han, Y., Mo, Y., Jiang, H., Cui, M., Jiang, B., Chen, Y., Tang, J., Song, J., Peng, P., and Zhang, G.: Molecular compositions and optical properties of dissolved brown carbon in biomass burning, coal combustion, and vehicle emission aerosols illuminated by excitation–emission matrix spectroscopy and Fourier transform ion cyclotron resonance mass spectrometry analysis, Atmos. Chem. Phys., 20, 2513-2532, https://doi.org/10.5194/acp-20-2513-2020, 2020b.

Wang, J., Jiang, H., Jiang, H., Mo, Y., Geng, X., Li, J., Mao, S., Bualert, S., Ma, S., Li, J., and Zhang, G.: Source apportionment of water-soluble oxidative potential in ambient total suspended particulate from Bangkok: Biomass burning versus fossil fuel combustion, Atmos. Environ., 235, 117624, https://doi.org/10.1016/j.atmosenv.2020.117624, 2020a.

Wang, K., Pang, Y., He, C., Li, P., Xiao, S., Sun, Y., Pan, Q., Zhang, Y., Shi, Q., and He, D.: Optical and molecular signatures of dissolved organic matter in Xiangxi Bay and mainstream of Three Gorges Reservoir, China: Spatial variations and environmental implications, Sci. Total Environ., 657, 1274-1284, https://doi.org/10.1016/j.scitotenv.2018.12.117, 2019.

Wang, X., Hayeck, N., Brüggemann, M., Abis, L., Riva, M., Lu, Y., Wang, B., Chen, J., George, C., and Wang, L.: Chemical Characteristics and Brown Carbon Chromophores of Atmospheric Organic Aerosols Over the Yangtze River Channel: A Cruise Campaign, J. Geophys. Res.-Atmos., 125, e2020JD032497, https://doi.org/10.1029/2020jd032497, 2020b.

Wong, J. P. S., Nenes, A., and Weber, R. J.: Changes in Light Absorptivity of Molecular Weight Separated Brown Carbon Due to Photolytic Aging, Environ. Sci. Technol., 51, 8414-8421, https://doi.org/10.1021/acs.est.7b01739, 2017.

Wu, C., Wang, G., Li, J., Li, J., Cao, C., Ge, S., Xie, Y., Chen, J., Li, X., Xue, G., Wang, X., Zhao, Z., and Cao, F.: The characteristics of atmospheric brown carbon in Xi'an, inland China: sources, size distributions and optical properties, Atmos. Chem. Phys., 20, 2017-2030, https://doi.org/10.5194/acp-20-2017-2020, 2020a.

Wu, F. C., Evans, R. D., and Dillon, P. J.: Separation and Characterization of NOM by High-Performance Liquid Chromatography and On-Line Three-Dimensional Excitation Emission Matrix Fluorescence Detection, Environ. Sci. Technol., 37, 3687-3693, https://doi.org/10.1021/es020244e, 2003.

Wu, G., Wan, X., Gao, S., Fu, P., Yin, Y., Li, G., Zhang, G., Kang, S., Ram, K., and Cong, Z.: Humic-Like Substances (HULIS) in Aerosols of Central Tibetan Plateau (Nam Co, 4730 m asl): Abundance, Light Absorption Properties, and Sources, Environ. Sci. Technol., 52, 7203-7211, https://doi.org/10.1021/acs.est.8b01251, 2018.

Wu, G., Ram, K., Fu, P., Wang, W., Zhang, Y., Liu, X., Stone, E. A., Pradhan, B. B., Dangol, P. M., Panday, A. K., Wan, X., Bai, Z., Kang, S., Zhang, Q., and Cong, Z.: Water-Soluble Brown Carbon in Atmospheric Aerosols from Godavari (Nepal), a Regional Representative of South Asia, Environ. Sci. Technol., 53, 3471-3479, https://doi.org/10.1021/acs.est.9b00596, 2019.

Wu, G., Wan, X., Ram, K., Li, P., Liu, B., Yin, Y., Fu, P., Loewen, M., Gao, S., Kang, S., Kawamura, K., Wang, Y., and Cong, Z.: Light absorption, fluorescence properties and sources of brown carbon aerosols in the Southeast Tibetan Plateau, Environ. Pollut., 257, 113616, https://doi.org/10.1016/j.envpol.2019.113616, 2020b.

Wu, G., Fu, P., Ram, K., Song, J., Chen, Q., Kawamura, K., Wan, X., Kang, S., Wang, X., Laskin, A., and Cong, Z.: Fluorescence characteristics of water-soluble organic carbon in atmospheric aerosol, Environ. Pollut., 268, 115906, https://doi.org/10.1016/j.envpol.2020.115906, 2021.

Xie, M., Chen, X., Holder, A. L., Hays, M. D., Lewandowski, M., Offenberg, J. H., Kleindienst, T. E., Jaoui, M., and Hannigan, M. P.: Light absorption of organic carbon and its sources at a southeastern U.S. location in summer, Environ. Pollut., 244, 38-46, https://doi.org/10.1016/j.envpol.2018.09.125, 2019.

Yan, C., Zheng, M., Sullivan, A. P., Bosch, C., Desyaterik, Y., Andersson, A., Li, X., Guo, X., Zhou, T., Gustafsson, Ö., and Collett, J. L.: Chemical characteristics and light-absorbing property of water-soluble organic carbon in Beijing: Biomass burning contributions, Atmos. Environ., 121, 4-12, https://doi.org/10.1016/j.atmosenv.2015.05.005, 2015.

Yan, C., Zheng, M., Desyaterik, Y., Sullivan, A. P., Wu, Y., and Collett Jr., J. L.: Molecular Characterization of Water-Soluble Brown Carbon Chromophores in Beijing, China, J. Geophys. Res.-Atmos., 125, e2019JD032018, https://doi.org/10.1029/2019jd032018, 2020.

Yan, G., and Kim, G.: Speciation and Sources of Brown Carbon in Precipitation at Seoul, Korea: Insights from Excitation-Emission Matrix Spectroscopy and Carbon Isotopic Analysis, Environ. Sci. Technol., 51, 11580-11587, https://doi.org/10.1021/acs.est.7b02892, 2017.

Yue, S., Ren, L., Song, T., Li, L., Xie, Q., Li, W., Kang, M., Zhao, W., Wei, L., Ren, H., Sun, Y., Wang, Z., Ellam, R. M., Liu, C. Q., Kawamura, K., and Fu, P.: Abundance and Diurnal Trends of Fluorescent Bioaerosols in the Troposphere over Mt. Tai, China, in Spring, J. Geophys. Res.-Atmos., 124, 4158-4173, https://doi.org/10.1029/2018jd029486, 2019.

Zhou, Y., Wen, H., Liu, J., Pu, W., Chen, Q., and Wang, X.: The optical characteristics and sources of chromophoric dissolved organic matter (CDOM) in seasonal snow of northwestern China, The Cryosphere, 13, 157-175, https://doi.org/10.5194/tc-13-157-2019, 2019.

Zsolnay, A., Baigar, E., Jimenez, M., Steinweg, B., and Saccomandi, F.: Differentiating with fluorescence spectroscopy the sources of dissolved organic matter in soils subjected to drying, Chemosphere, 38, 45-50, https://doi.org/10.1016/S0045-6535(98)00166-0, 1999.

Supplement of

Measurement report: Long emission-wavelength chromophores dominate the light absorption of brown carbon in Aerosols over Bangkok: impact from biomass burning

Jiao Tang et al.

Correspondence: Guangcai Zhong (gczhong@gig.ac.cn)

Content of this file

Text S1 to S4

Table S1 to S5

Figure S1 to ~~S16~~S17

Text S1. Analysis of carbon content

The concentration of WSOC was quantified using a TOC analyzer (Vario TOC cube; Elementar). All WSOC concentrations were blank corrected. The concentration of OC in MSOC was calculated as the difference between the OC and WSOC concentrations. The calculation assumed that all water-insoluble organic carbon in the aerosols can be extracted with methanol (Cheng et al., 2016). Chen et al. (2019) reported that only a small amount of organic carbon (OC, 6%) were extracted with DCM after water and methanol extraction, thus we assumed that methanol can extract the majority of the extractable OC in the aerosols.

Text S2. Analysis of UV-visible Absorption spectra

Absorption Ångström exponent (AAE) represents the wavelength dependence of absorption is calculated according to following formula (Fan et al., 2018):

$$A = K \bullet \lambda^{-AAE} \quad (1)$$

Here, A is the measured absorbance, and K is constant. 330 nm to 400 nm is selected for fitting AAE value.

Light absorption coefficient (Abs_λ, Mm^{-1}) can be calculated using the following formula (Yan et al., 2015):

$$Abs_\lambda = \frac{(A_\lambda - A_{700}) \times V_1 \times a \times \ln(10)}{Va \times a_1 \times l} \quad (2)$$

Here, A_λ is the value of light absorption at the given wavelength given by the spectrophotometer; V_1 and a_1 is the volume of ultra-pure deionized water or methanol for extraction and area of the extracted filter; Va is the volume of sampling air; l is the optical path length.

Mass absorption efficiency (MAE, $m^2\ g^{-1}$ C) can be obtained as follows (Cheng et al., 2011):

$$MAE_\lambda = \frac{Abs_\lambda}{C_i} \quad (3)$$

Here, C_i ($\mu g\ C/m^3$) is the concentration of WSOC and MSOC after conversion to the atmosphere. Moreover, the pH was measured for all samples within the range of 5–7, generally thought it didn't affect the absorbance according to prior study (Chen et al., 2016a).

To understand the importance of BrC in radiative forcing, its relative light absorption contribution to total aerosols was estimated by assuming that BrC and BC externally mixed in aerosols (Cheng et al., 2011). The relative contribution of each aerosol extract to the total light-absorption by the organics and EC was assessed. The total light-absorptions of the different aerosol extracts and EC were calculated from the MAEs of the organics and EC and their atmospheric concentrations using the following equation:

$$\mathrm{Abs}_{\lambda,total} = \sum_i MAE_{\lambda,i} \cdot C_i + MAE_{\lambda,EC} \cdot C_{EC} \quad (4)$$

where C_i is the concentration of the organics in extract i (i.e., WSOC, and MSOC) when they were in the atmosphere (μg C m^{-3}). The concentrations of C_{EC} were measured by thermal-optical (or thermal) method is typically used as BC (Cheng et al., 2011). The MAE of EC in the range of 250–700 were calculated, and MAE in the aerosols is expressed as a function of AAE (Chen et al., 2016a;Lee et al., 2014;Andreae and Gelencsér, 2006):

$$MAE_\lambda = a \cdot \lambda^{-AAE} \quad (5)$$

where a is a constant that is related to the light-absorptivity; the AAE values and MAE of EC at 550 nm assumed to be 1 and 7.5 m^2 g^{-1}, respectively (Bond and Bergstrom, 2006). And the variability of MAE and AAE is considered as 6.3–8.7 and 0.8–1.4, respectively (Liu et al., 2018a;Chen et al., 2016a;Bond and Bergstrom, 2006).

Figure S12 showed the relative contributions of each of the aerosol extracts to the total light absorption of the aerosols. In the low-UV region (250–300 nm), the light absorption of WSOC and MSOC fractions was higher than that of BC. At 250 nm, the light absorption of extracted BrC is as large as 35 Mm^{-1}, which is 1.5 times higher than the BC, and decreased to 19 Mm^{-1} at 300 nm with comparable values to the light absorption by BC. Although the significant UV absorption at wavelengths below 300 nm may not be important for the transfer of total solar radiation in the troposphere, the presence of light-absorbing organic aerosols may cause a reduction in UV photolysis and the near-surface ozone mixing ratios (Barnard et al., 2008). By contrast, the total light absorption by WSOC and MSOC is only 7.3 Mm^{-1} at 365 nm, accounting for an average of 28% of total light absorption. Xie et al. (2019a) observed higher contributions of BrC to the total absorption at 370 nm at ground level and 260m, on average accounting for 46% and 48%, respectively. In the visible region (400–600 nm), the extracted BrC contributed from an average of 21% of total absorption at 400 nm to 8.0% at 500 nm to below 4.0% at 600 nm and decreased continuously toward longer wavelengths. Hoffer et al. (2006) estimated that the contribution of HULIS to light absorption was only a few percent in Amazonia biomass burning aerosols at 532 nm and 35%–50% at 300 nm. Wu et al. (2019) reported water-soluble BrC contributed 25.3% of total light absorption at 300 nm by aerosols from Godavari, which was lower than our result (35%±11%). However, it should be noted that the measured absorption of BrC in extracts may be underestimated by a factor of about 2 than that in ambient conditions due to incomplete extraction of OC by solvents and size-dependent absorption properties of organic aerosol (Shetty et al., 2019;Liu et al., 2013). Although a large amount of BrC were extracted by ultra-pure deionized water, and then methanol, there were non- and low-polar compounds that could not extracted by the two solvents, such as aliphatic hydrocarbon structures, phthalate esters, and some polycyclic

aromatic hydrocarbons (Chen et al., 2017b). Thus, the actual absorption contribution of BrC in ambient conditions may be higher than the estimate of this study.

Generally, the AAE of BC particles is widely accepted to be 1.0, and this value was applied to calculate the MAE of BC in this study. However, a previous study reported BC AAE is not 1.0, even when BC is assumed to have small sizes and a wavelength-independent refractive index (Liu et al., 2018a), and vary from 0.8 to 1.4. The $MAE_{550,BC}$ is 7.5 m^2 g^{-1} at 550 nm for uncoated particles referring to previous study and the standard deviation is 1.5 m^2 g^{-1}(Bond and Bergstrom, 2006), which is used to calculate the MAE of BC at a different wavelength. Thus, the uncertainty of light absorption of BC in the studied wavelength of 250–700 nm was calculated from 13% to 44%.

Text S3. Quantifying spectral similarity

The Tucker congruence coefficient (TCC) is used for identifying similar spectra (Murphy et al., 2014), which increase its sensitivity to shape differences and peak shifts (Wünsch et al., 2019).

$$\mathrm{TCC}\ (x, y) = \frac{\sum x\, y}{\sqrt{\sum x^2 \sum y^2}} \quad (6)$$

Where x and y are loading of two factors with identical x-axis-scale. TCCs are calculated for emission and excitation spectra (TCC_{ex} and TCC_{em}) to form the overall $TCC_{em\times ex}$. TCC which is higher than 0.95 means high similarity.

Text S4. Quality control

In this study, the relative standard deviation of WSOC concentration of parallel experiments of ambient particle samples based on method and instrument were 2.8% and 0.3%–4.6%. The error of WSOC concentration in five blank samples was 8.3%. The error of OC with value of 5.5% is presented in previous study (Wang et al., 2020). Thus, the calculated error of MSOC concentration is 10%. We corrected the procedural blank concentrations of WSOC concentration.

The value of absorbance of WSOC for field blank samples at 365 nm was 0.00063, and that of MSOC was lower than method detection limit (MDL). MDL was calculated based on the average of three blank samples at 365 nm adding the three times standard deviation, with values of 0.00057 and 0.00014 for WSOC and MSOC, respectively. The standard deviation of three-group parallel experiments of absorbance at 250–700nm were 0.00015±0.00013, 0.0095±0.0091, and 0.00002±0.00002. Further, no obvious peak was found in the fluorescence spectrum of field blank samples. The fluorescence spectrum of samples was measured with their absorbance lower than 1.

Table S1 The average meteorological data (mean±S. D.) in different seasons over Bangkok in Thailand from January 2016 to January 2017.

	Month	Temperature (° F)	Humidity (%)	Wind Speed (mph)	Pressure
Pre-hot season	Jan.–Feb.	82±5.0	67±11	6.2±1.9	30±0.067
Hot season	Mar.–May.	89±2.5	68±7.3	8.8±1.4	30±0.12
Monsoon	Jan, and Oct.	84±2.2	81±8.2	6.2±1.6	30±0.059
Cool season	Nov. –Jan.	83±2.4	70±8.1	6.0±1.4	30±0.058

Table S2 Fluorescent components identified by parallel factor analysis (PARAFAC) in water-soluble organic carbon (WSOC) and methanol-soluble organic carbon (MSOC) in aerosol samples over Bangkok, Thailand (85-model), and their Tucker congruence coefficient (TCC) values with components of 145-model containing ambient aerosol samples and source samples.

Components (85-model)	Excitation maxima (nm)	Emission maxima (nm)	Assignment according to previous studies	145-model components	TCC values	References
P1	290	356	Protein-like fluorophore	145M-P3	0.94	(Qin et al., 2018;Fan et al., 2016)
P2	<250/308	415	Humic-like substances	145M-P1	0.97	(Chen et al., 2017a;Stedmon and Markager, 2005;Wu et al., 2019)
P3	254/356	443	The fluorescence of aqueous reactions of hydroxyacetone with glycine, or humic-like substances	145M-P6	0.90	(Gao and Zhang, 2018;Chen et al., 2003)
P4	257/386	513	Humic-like substances	145M-P5	0.96	(Chen et al., 2017a;Stedmon and Markager, 2005;Wu et al., 2019)
P5	<250	383		145M-P4	0.97	

P6	<250/332	392	N-containing SOA species, pyridoxine, or humic-like substances	145M-P7	0.97	(Babar et al., 2017;Pohlker et al., 2012;Chen et al., 2003)
P7	278	310	Tyrosine-like fluorophore, non-N-containing species	145M-P8	0.90	(Chen et al., 2016b;Zhou et al., 2019)
C1	<250	434	Fulvic acid-like substances	145M-C1	0.99	(Chen et al., 2003)
C2	<250	383	Fulvic acid-like substances	145M-C3	0.99	(Chen et al., 2003)
C3	287	351		145M-C2	0.97	
C4	260	513		145M-C4	0.97	
C5	<250	360		145M-C5	0.93	
C6	275	306	Tyrosine-like fluorophore	145M-C7	0.98	(Stedmon and Markager, 2005)

114

115 **Table S3** Comparisons of light absorption of aerosol samples from Bangkok with the other studies.

Samples	Sites	Fraction	AAE	MAE_{365} (m^2 g^{-1} C)	References
TSP	Thailand	Water-soluble BrC	5.1±0.68	0.83±0.25	This study
		Methanol-soluble BrC	5.2±0.94	0.26±0.12	
PM_{10}	Nepal	Water-soluble BrC		0.59 ± 0.16 in the monsoon season 1.05 ± 0.21 in the pre-monsoon season	(Wu et al., 2019)
$PM_{2.5}$	Beijing	Water-soluble BrC	5.30 ± 0.44 in winter 5.83 ± 0.51 in summer	1.54 ± 0.16 in winter 0.73 ± 0.15 in summer	(Yan et al., 2015)
TSP	Guangzhou	Water-soluble BrC	5.33±0.71	0.81±0.16	(Liu et al., 2018b)
$PM_{2.5}$	Beijing	Water-soluble BrC		1.79±0.24 in winter 0.71±0.20 in summer	(Cheng et al., 2011)

$PM_{2.5}$		Water-soluble BrC		0.76	(Chen et al., 2018)
$PM_{2.5}$	Southeastern US	Water-soluble BrC		0.29±0.13	(Xie et al., 2019b)
$PM_{2.5}$	South Asia	Water-soluble BrC	4.00–4.44 in Deihi 5.11–6.68 in BCOB 6.63–7.13 in MCOH	2.24–2.49 in Deihi 1.35–1.45 in BCOB 0.31–0.52 in MCOH	(Dasari et al., 2019)
$PM_{2.5}$	Beijing	Water-soluble BrC	5.27 ± 0.81	1.05 ± 0.32	(Mo et al., 2018)
$PM_{2.5}$	Simulated biomass burning	Water-soluble BrC	7.40–9.03	0.86–1.23	(Fan et al., 2018)
$PM_{2.5}$	Simulated biomass burning	Water-soluble BrC		0.76–1.44	(Park and Yu, 2016)
TSP	Simulated biomass burning	Water-soluble BrC	7.1±1.6	1.6 ± 0.55	(Tang et al., 2020b;Tang et al., 2020a)
	Simulated anthracite combustion	Water-soluble BrC		1.3 ± 0.34	
	Vehicle emission	Water-soluble BrC		0.71 ± 0.30	
	Simulated biomass burning	Methanol-soluble BrC		2.3 ± 1.1	
	Simulated anthracite combustion	Methanol-soluble BrC		0.88 ± 0.74	
	Vehicle emission	Methanol-soluble BrC		0.26 ± 0.09	

Table S4 Summary of multiple linear regression results between light absorption at 365 nm (Abs_{365}, Mm^{-1}) of water-soluble BrC and its individual fluorescent chromophore identified by parallel factor analysis in aerosol samples over Bangkok.

Model	Unstandardized coefficients		Standardized coefficients	t-STAT	p-Value
	B	Standard error	Beta		
Regression 1: n=85, R^2 = 0.994, Adjust R^2 = 0.994, error=0.38295					
P4 component	0.923	0.008	0.997	117.85	0.000
Regression 2: n=85, R^2 = 0.994, Adjust R^2 = 0.994, error=0.37123					
P4 component	0.898	0.013	0.97	71.382	0.000
P2 component	0.02	0.008	0.034	2.515	0.014

Regression 3: n=85, R^2 = 0.995, Adjust R^2 = 0.995, error=0.36385					
P4 component	0.765	0.065	0.826	11.767	0
P2 component	0.051	0.017	0.088	3.033	0.003
P7 component	0.091	0.044	0.107	2.088	0.04
Regression 4: n=85, R^2 = 0.995, Adjust R^2 = 0.995, error=0.35652					
P4 component	0.979	0.121	1.057	8.104	0
P2 component	0.041	0.017	0.071	2.399	0.019
P7 component	0.14	0.049	0.165	2.875	0.005
P3 component	-0.164	0.079	-0.275	-2.089	0.04

Note: Pre multiple linear regression (MLR), curve estimation was conducted to estimate the possible correlations between the dependent and independent variables. Statistical parameters were computed as the goodness-of-fit indicators including adjusted R^2, t-STAT (ratio of coefficient to standard error), *p*-value (target < 0.05). For the independent variables with significant correlations with the dependent variable (*p*-value < 0.05), or with positive contributions to the independence, Abs_{365}, they will be retained in the statistical model as the efficiency factors to the Abs_{365}. To simplify the model, non-significant independences, as well as constant, were gradually removed.

Table S5 Summary of multiple linear regression results between light absorption at 365 nm (Abs_{365}, Mm^{-1}) of methanol-soluble BrC and its individual fluorescent chromophore identified by parallel factor analysis in aerosol samples over Bangkok.

Model	Unstandardized coefficients		Standardized coefficients	t-STAT	p-Value
	B	Standard error	Beta		
Regression 1: n=85, R^2 = 0.945, Adjust R^2 = 0.944, error=0.33609					
C4 component	0.238	0.006	0.972	37.738	0.000
Regression 2: n=85, R^2 = 0.957, Adjust R^2 = 0.956, error=0.29861					
C4 component	0.489	0.052	1.998	9.317	0.000
C1 component	-0.119	0.025	-1.032	-4.811	0.000

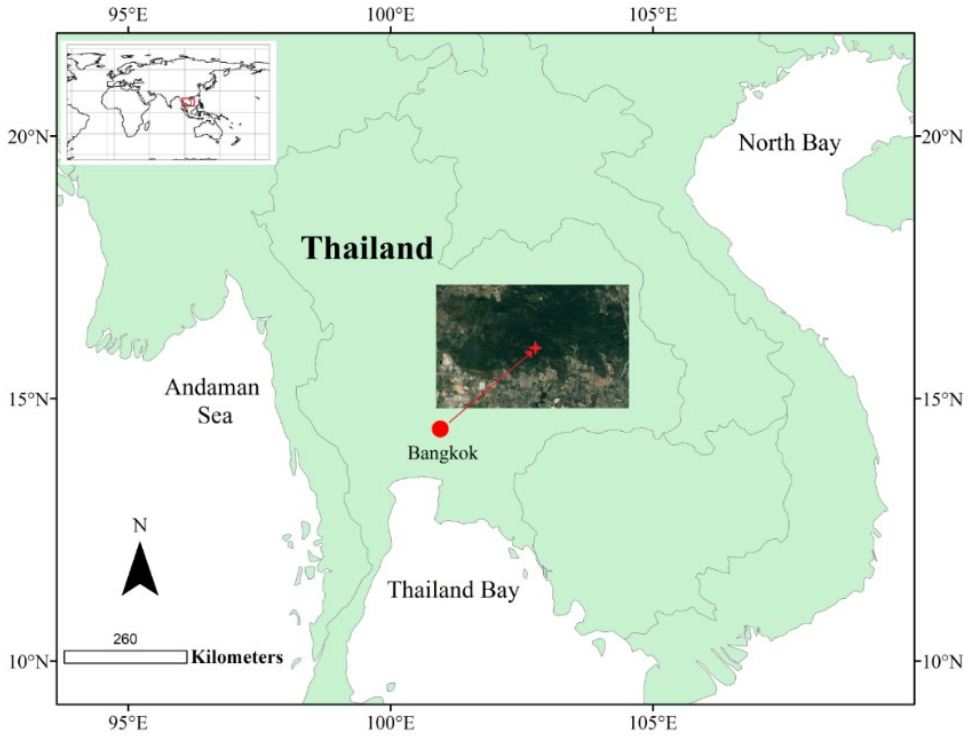

Figure S1. Location of sampling site at the faculty of the environment of Kasetsart University in Bangkok, Thailand. The basemap was drawn by ArcGIS software (ESRI Inc. California, USA). The satellite image at the center was derived from Google Maps (Image © Google Maps 2019).

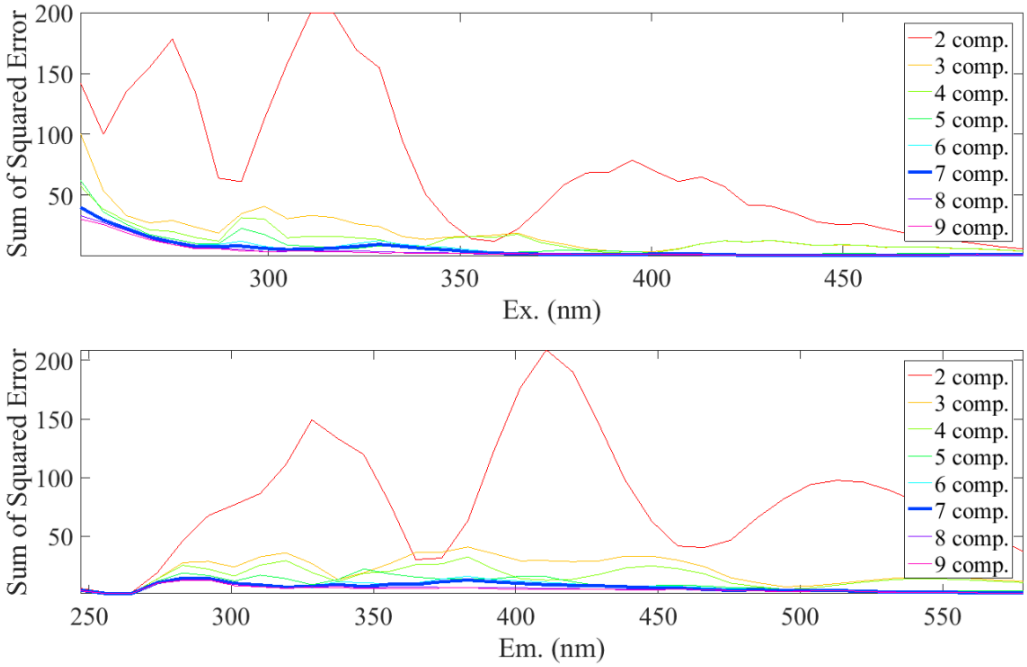

Figure S2. Sum of squared error of excitation and emission wavelength for 2–9 PARAFAC model in the WSOC in aerosol samples from Bangkok (n=85).

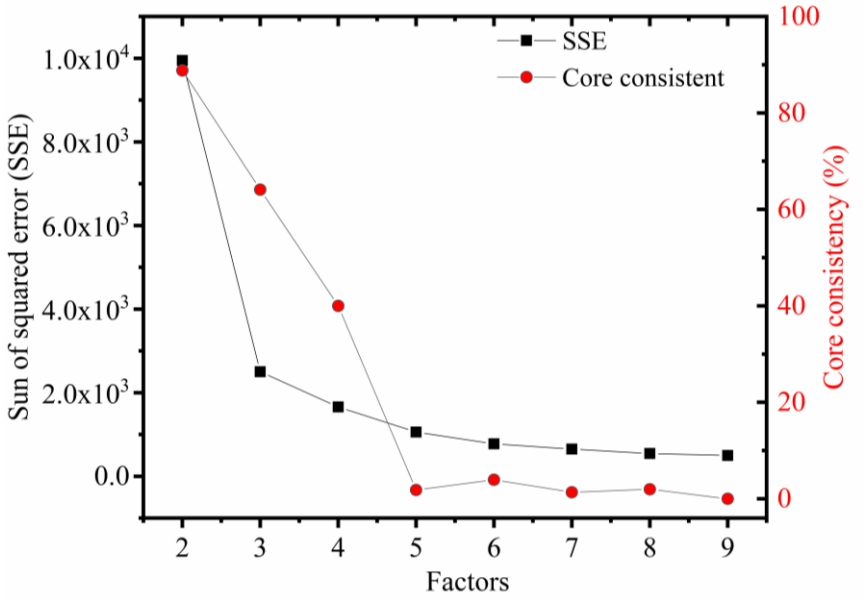

Figure S3. Sum of squared error (SSE) and core consistency of each PARAFAC model in the WSOC in aerosol samples from Bangkok (n=85).

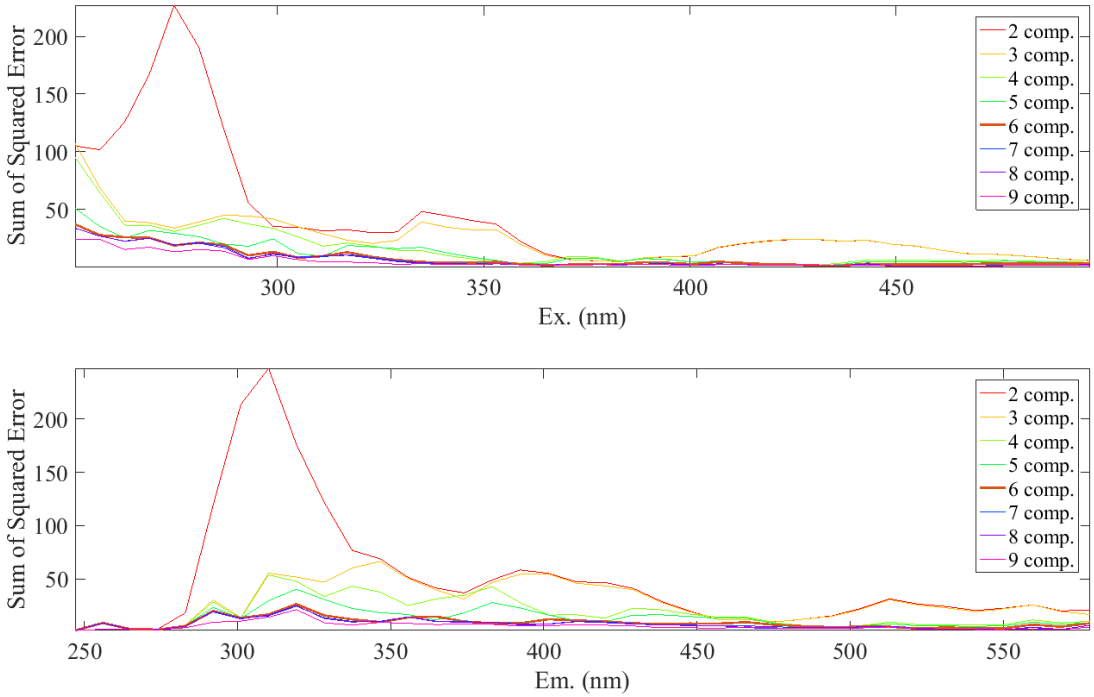

Figure S4. Sum of squared error of excitation and emission wavelength for 2–9 PARAFAC model in the MSOC fraction in aerosol samples from Bangkok (n=85).

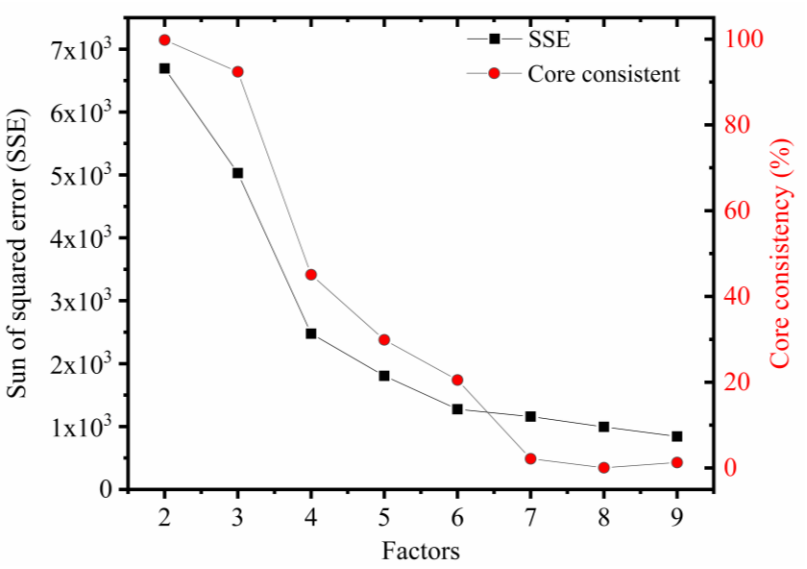

Figure S5. Sum of squared error (SSE) and core consistency of each PARAFAC model in the MSOC in aerosol samples from Bangkok (n=85).

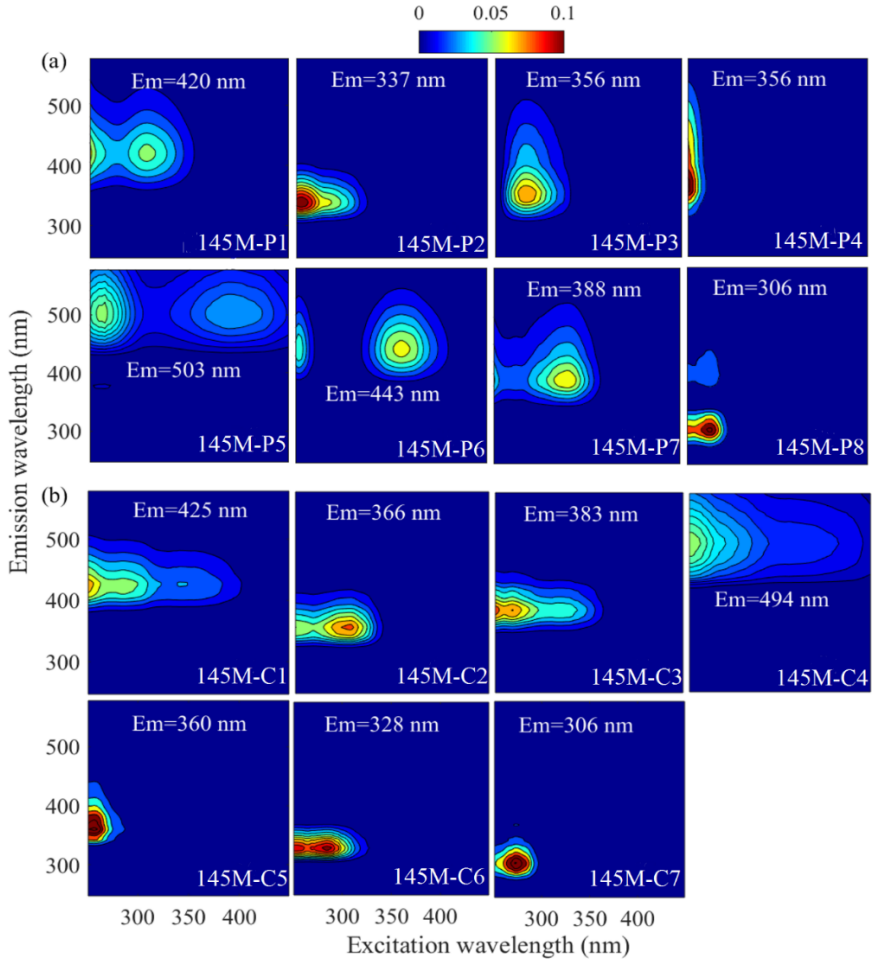

Figure S6. The eight fluorescent components of the WSOC (a, 145-model, 145M-P1–8) and seven fluorescent components of the MSOC (b, 145-model, 145M-C1–8), respectively, identified by the PARAFAC method in aerosol samples from Bangkok, Thailand, and source samples (n=145).

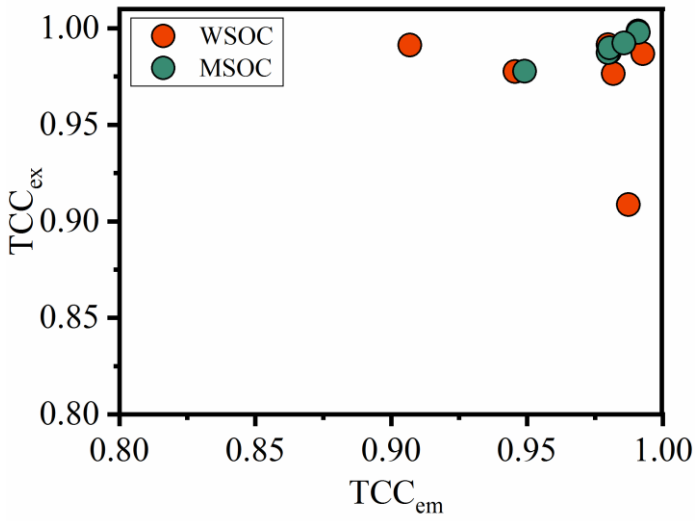

Figure S7. Evaluation of fluorescence emission and excitation spectrum similarity of 85-model with 145-model by Tucker congruence coefficient (TCC).

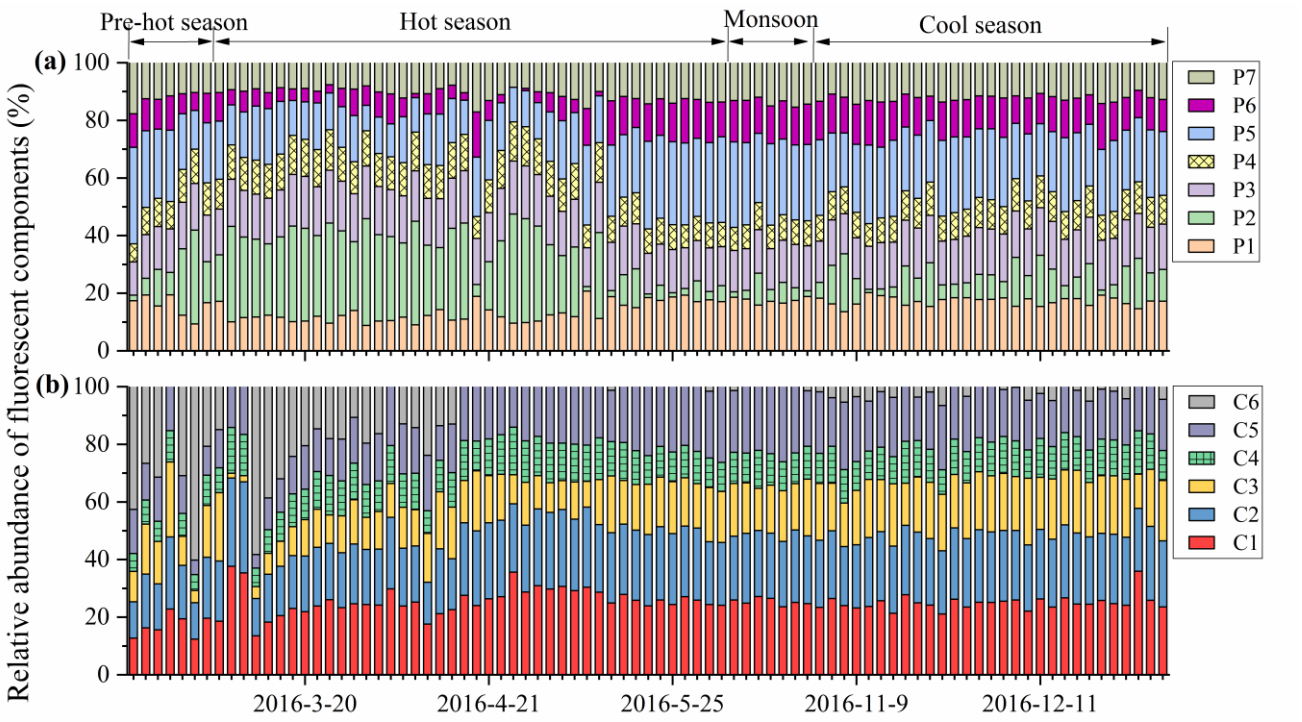

Figure S8. Relative abundances of the PARAFAC-derived components of WSOC (a, P1–7) and MSOC (b, C1–6) of aerosol samples over Bangkok in Thailand (85-model). Pre-hot season is from January 18 to February 29, 2016; hot season is from March 2 to May 31, 2016; monsoon is from June 2 to October 30, 2016; cool season is from November 1, 2016 to January 28, 2017.

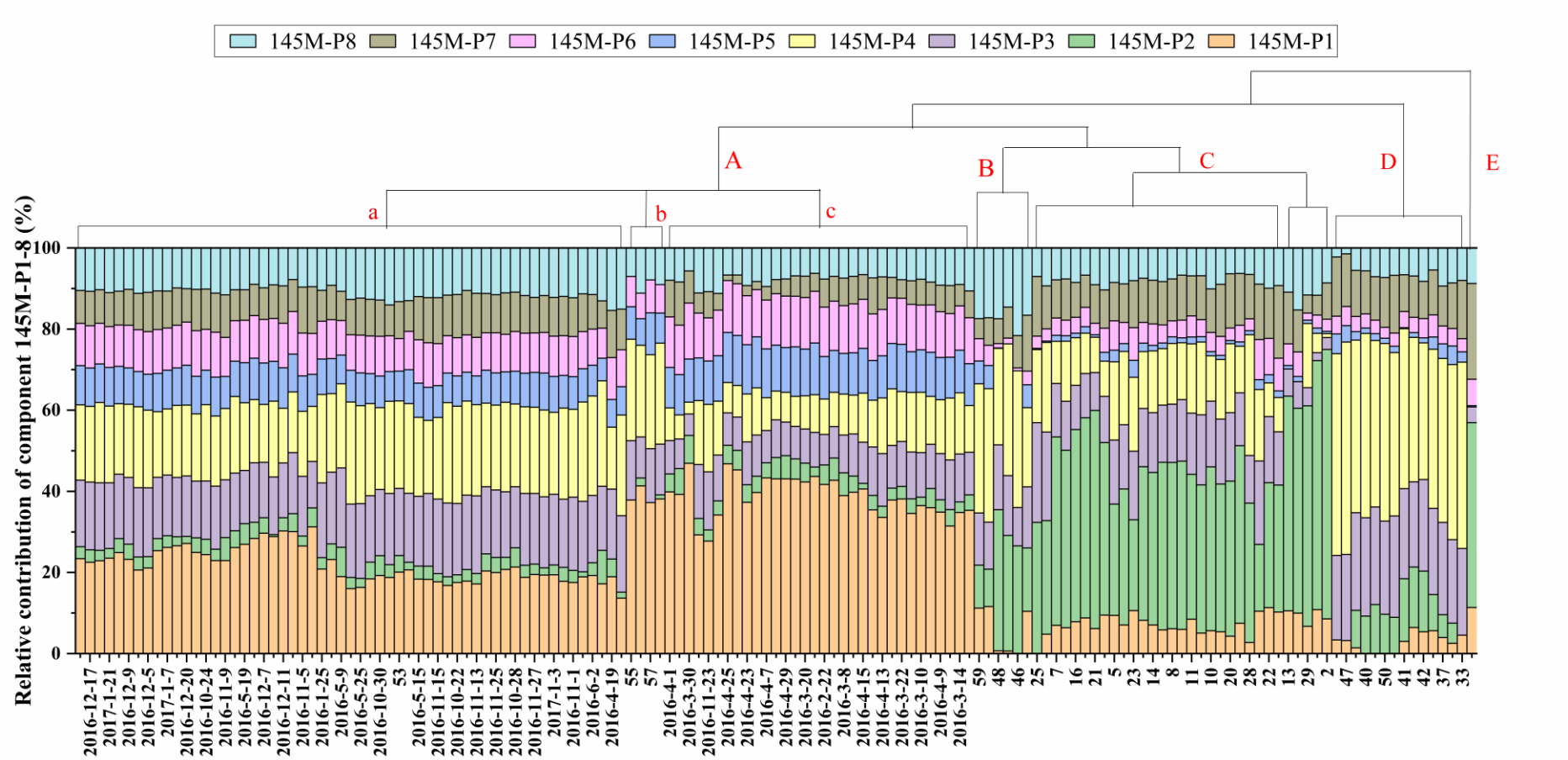

Figure S9. Hierarchical cluster analysis based on the relative contributions of PARAFAC-derived components (145-model, 145M-P1–8) in the WSOC. The sample IDs correspond to different types of aerosols as follows: ID 1–33: aerosol samples from simulated biomass burning; ID 34–50: aerosol samples from simulated coal combustion; ID 51–58: aerosol samples collected in the tunnel; ID 59–60: aerosol samples from vehicle exhaust.

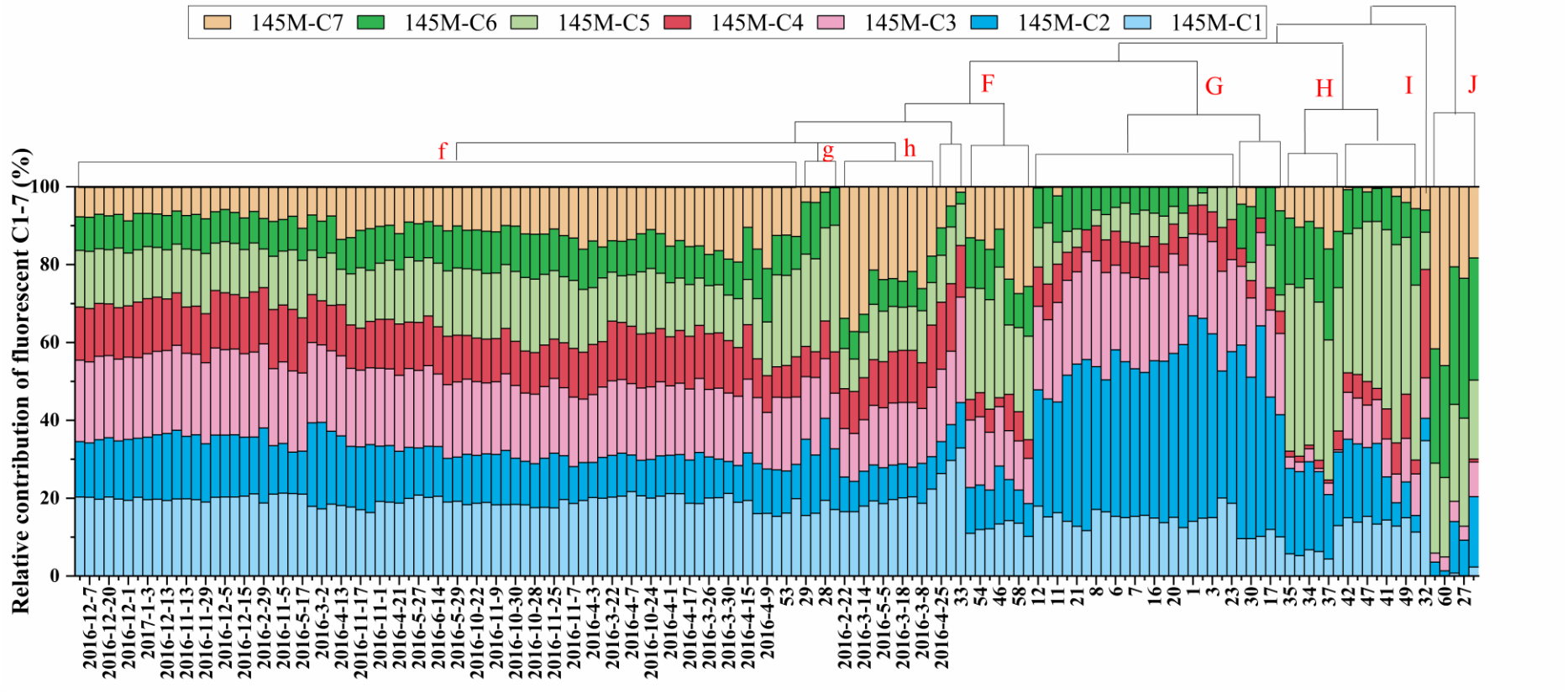

Figure S10. Hierarchical cluster analysis based on the relative contributions of PARAFAC-derived components (145-model, 145M-C1–7) in the MSOC. The sample IDs correspond to different types of aerosols as follows: ID 1–33: aerosol samples from simulated biomass burning; ID 34–50: aerosol samples from simulated coal combustion; ID 51–58: aerosol samples collected in the tunnel; ID 59–60: aerosol samples from vehicle exhaust.

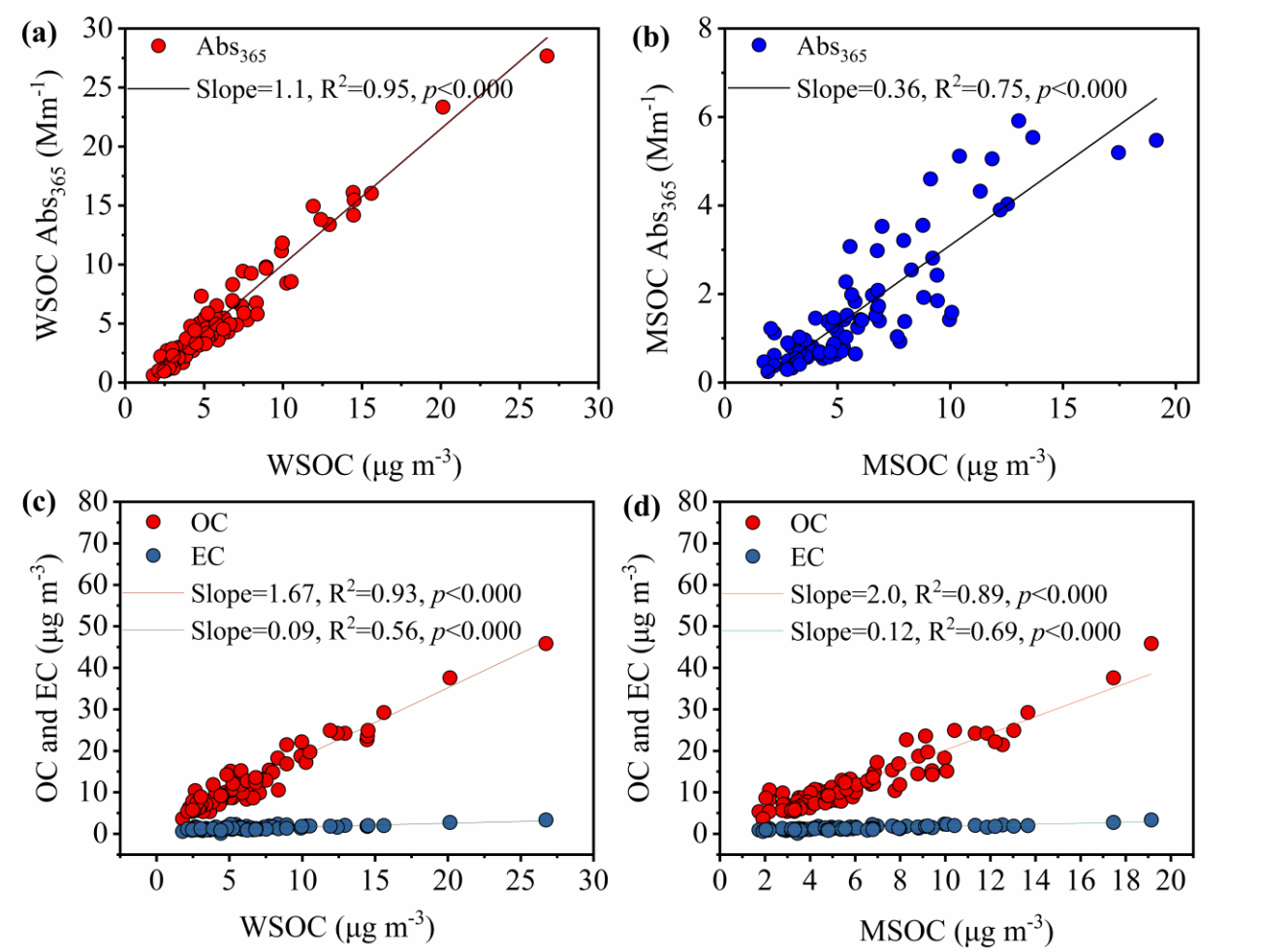

Figure S11. Scatter plots of Abs_{365} (Mm^{-1}) of water-soluble BrC versus WSOC (μg C m^{-3}) (a) and Abs_{365} (Mm^{-1}) of methanol-soluble BrC versus MSOC (μg C m^{-3}) (b), and WSOC versus OC and EC (c) and MSOC versus OC and EC (d) in aerosol samples from Bangkok, Thailand, respectively. Where the slope (a and b) is defined as the WSOC or MSOC mass absorption efficiency (MAE, solvent extract absorption at 365 nm per WSOC or MSOC mass m^2 g^{-1} C).

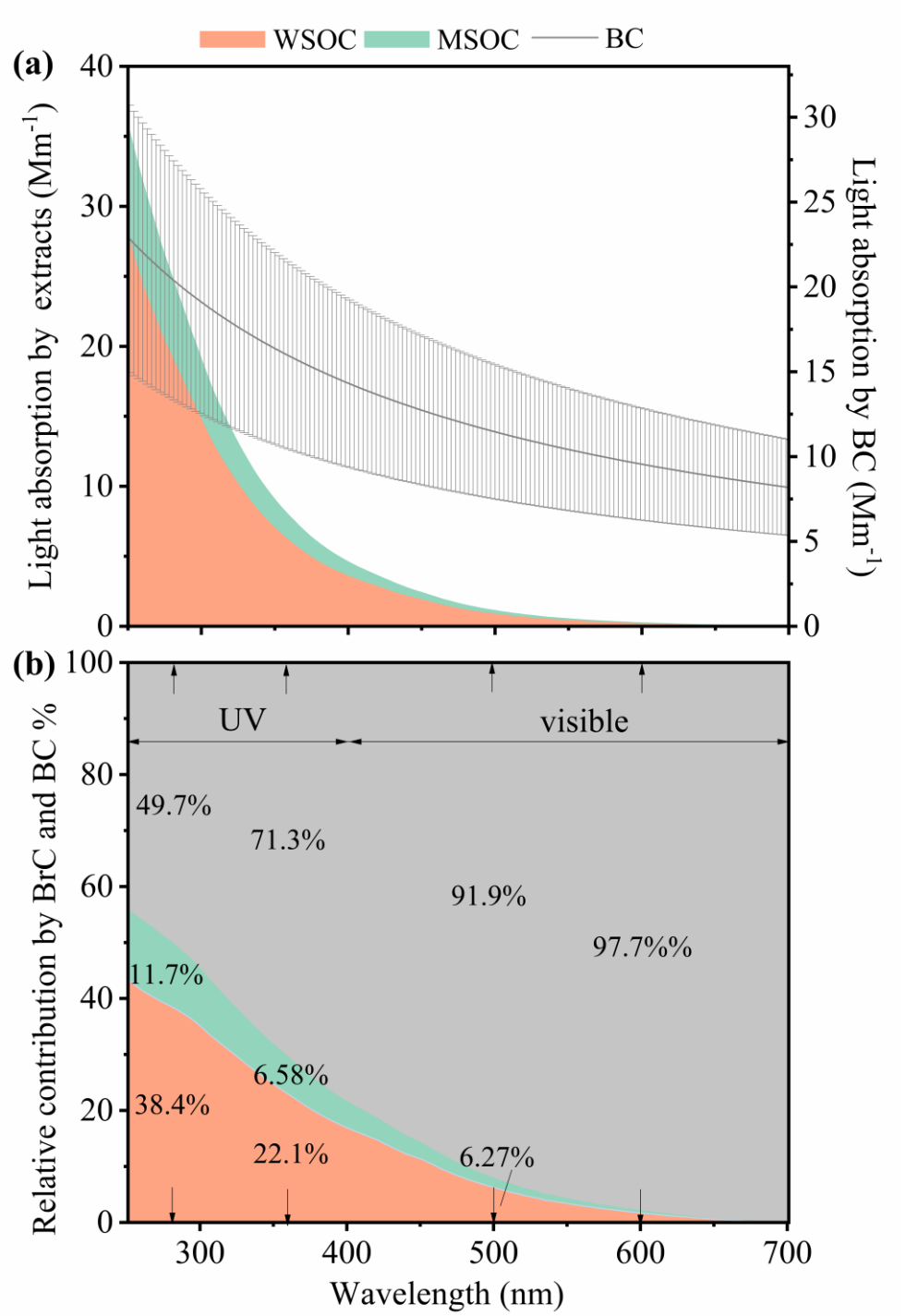

Figure S12. Mean light absorption of water-soluble BrC, methanol-soluble BrC, and BC (a), and relative to total light-absorption aerosol (b) in the aerosol samples from Bangkok during 2016-2017.

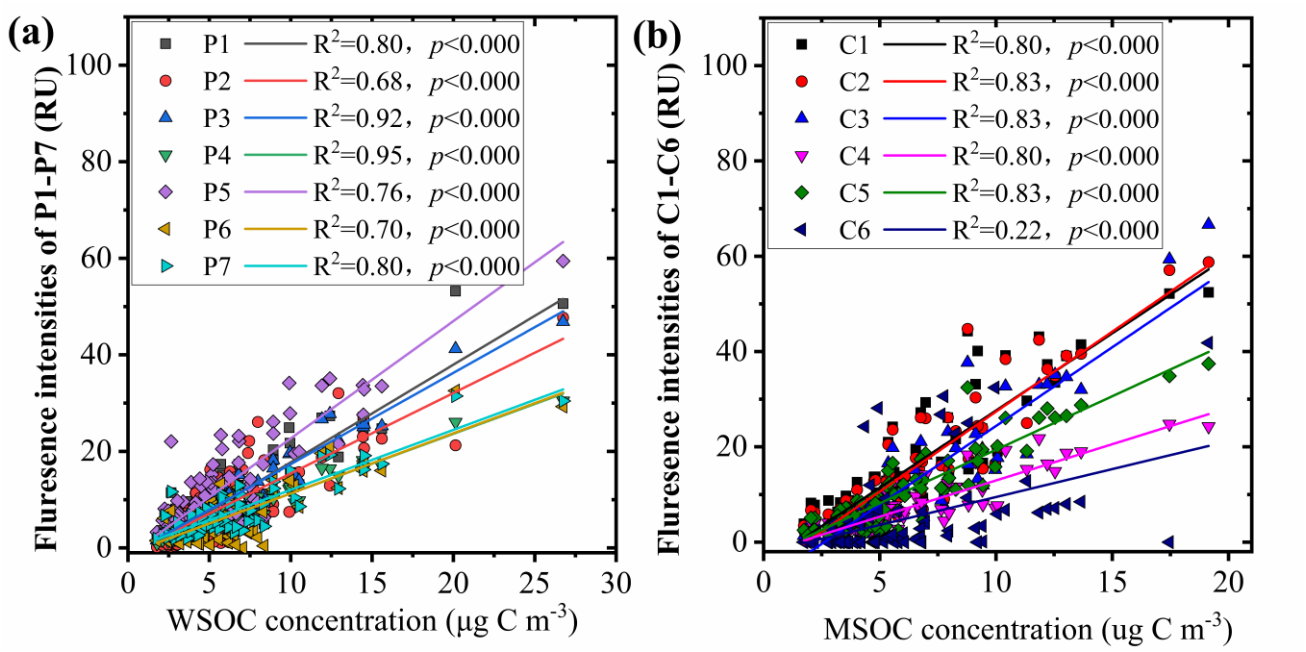

186

187 **Figure S13.** Scatter plots of (a) WSOC concentration (μg C m^{-3}) versus fluorescence intensities of component P1–
188 P7 (RU) in the WSOC fraction and (b) MSOC concentration (μg C m^{-3}) versus fluorescence intensities of component
189 C1–C6 (RU) in the MSOC fraction in aerosol samples over Bangkok.

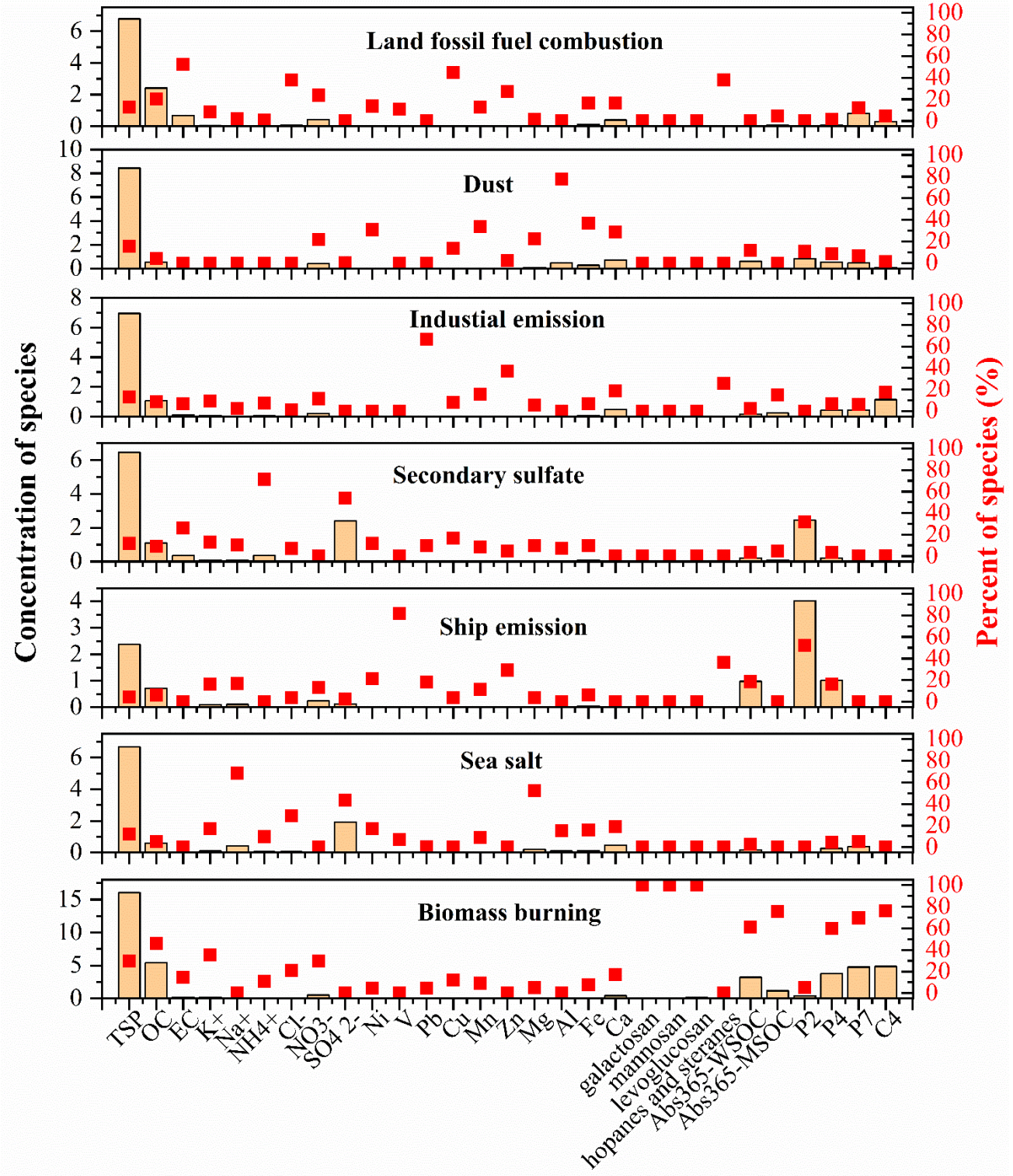
Land fossil fuel combustion
Dust
Industial emission
Secondary sulfate
Ship emission
Sea salt
Biomass burning
Concentration of species
Percent of species (%)
TSP
OC
EC
K+
Na+
NH4+
Cl-
NO3-
SO4 2-
Ni
V
Pb
Cu
Mn
Zn
Mg
Al
Fe
Ca
galactosan
mannosan
levoglucosan
hopanes and steranes
Abs365-WSOC
Abs365-MSOC
P2
P4
P7
C4

190

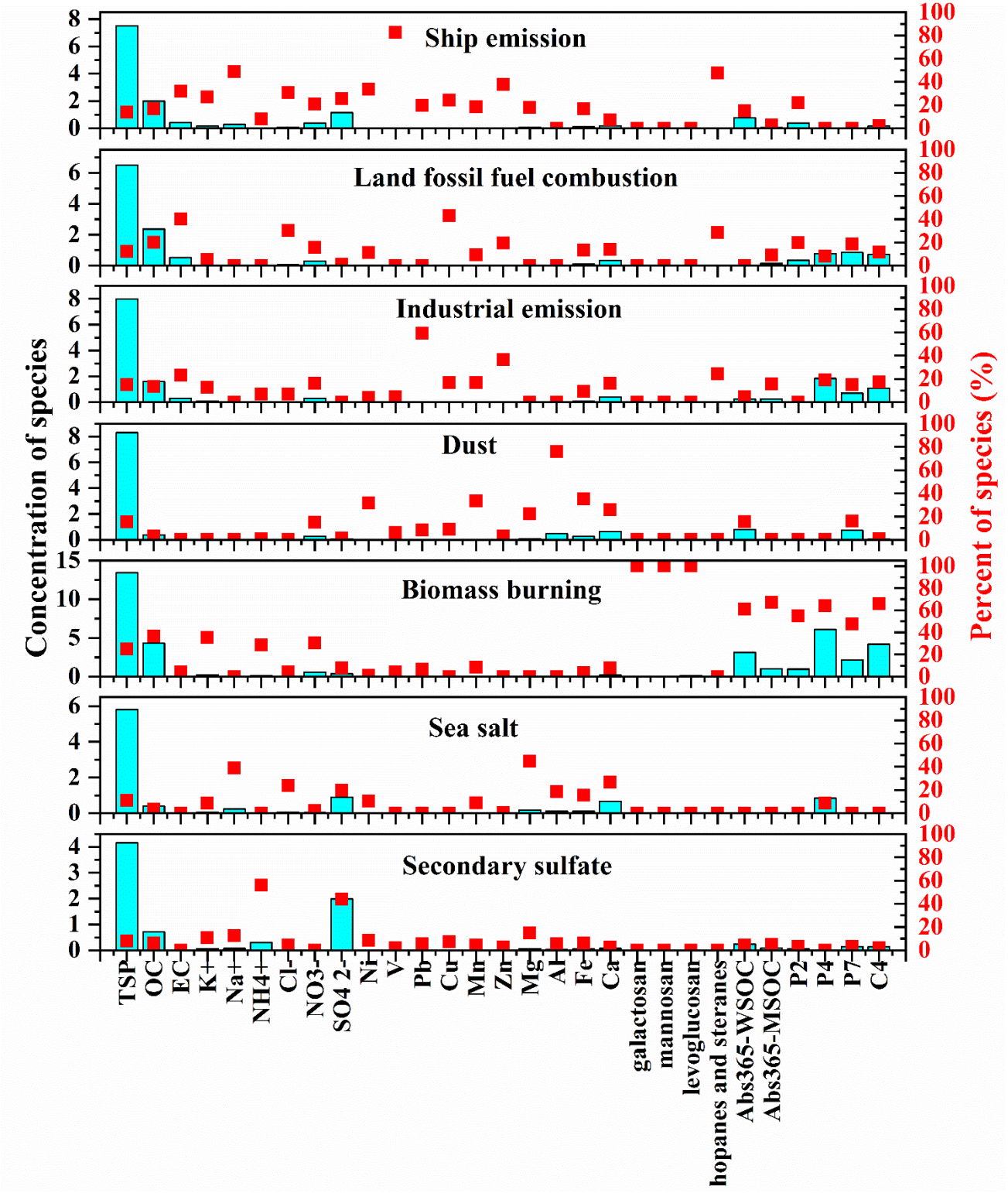

Figure S14. Factor profiles resolved by positive matrix factorization mode. The bars represent the concentrations of species and the dots represent the contributions of species appointed to the factors. The run method was detailly described elsewhere (Wang et al., 2020).

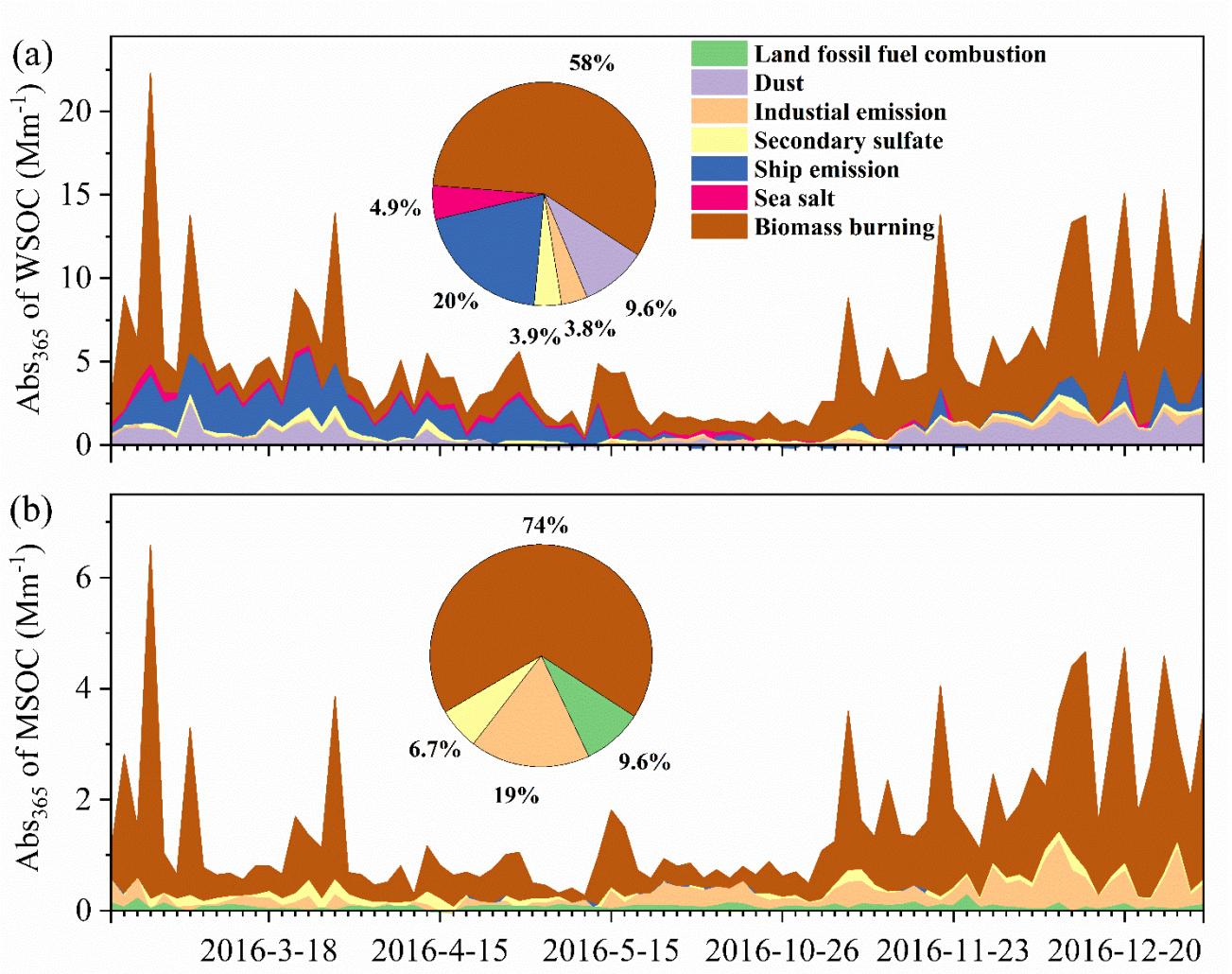

197

198 **Figure S15.** The time-series of absorption at 365nm of the WSOC (a), and of the MSOC (b) in TSP samples over

199 Bangkok contributed by each factor resolved by positive matrix factorization.

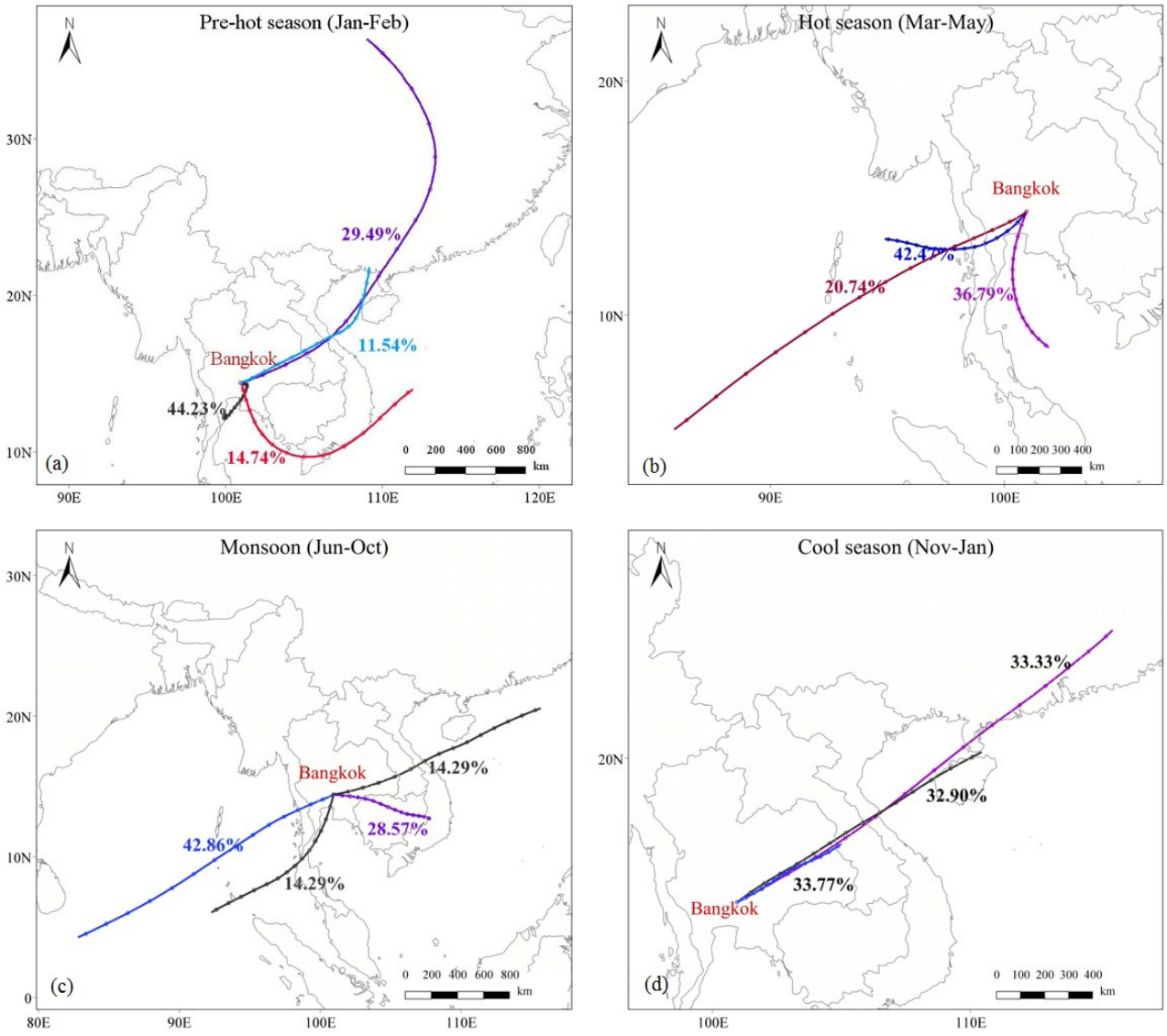

Figure S15S16. The 72 h back air-mass trajectories at Bangkok from Thailand during the (a) pre-hot season (January to February 2016), (b) hot season (March to May 2016), (c) monsoon (June to October in 2016), (d) cool season (November 2016 to January 2017). The air-mass trajectories were analyzed by HYSPLIT model.

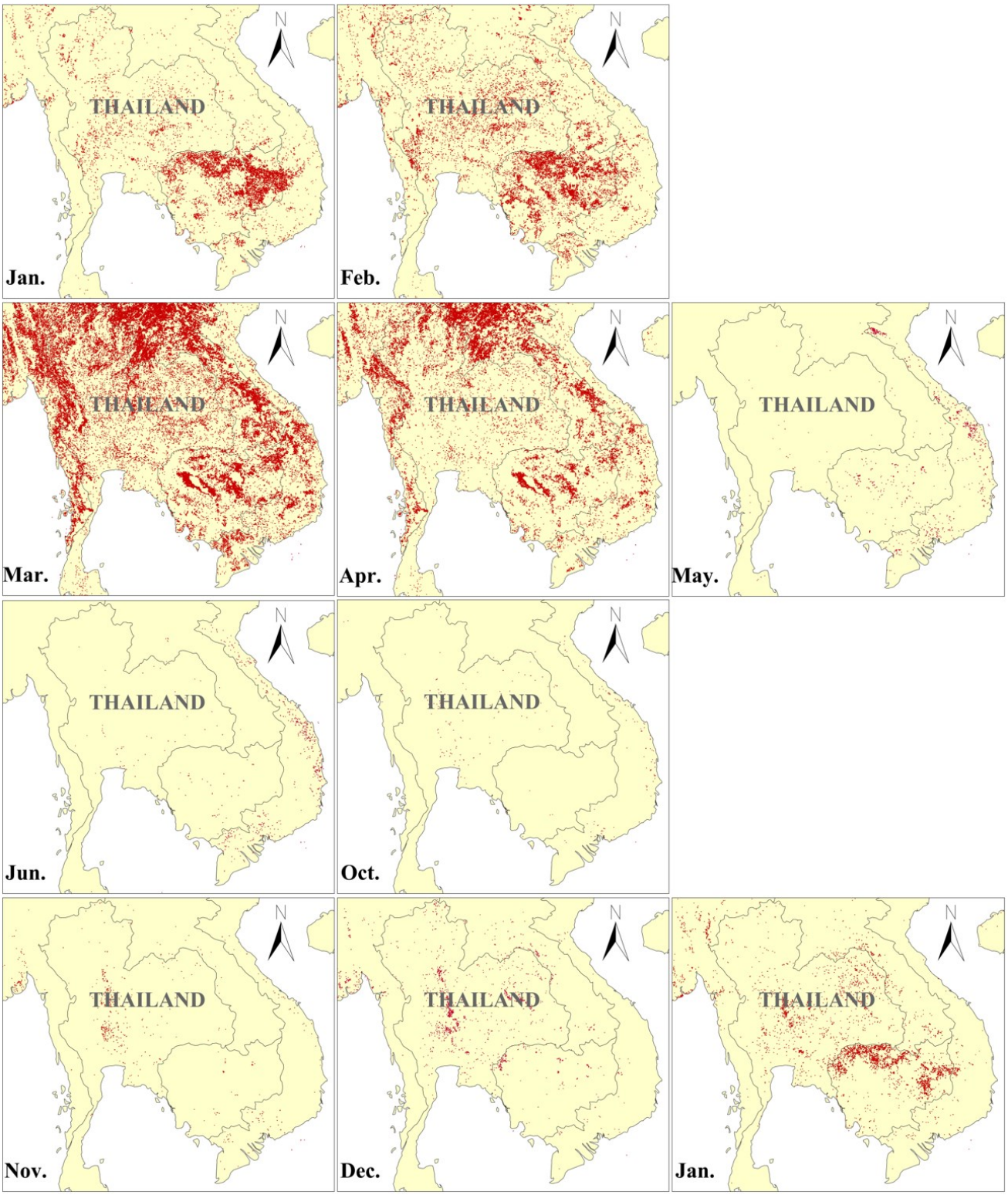

Figure ~~S16~~S17. The spatial distribution of active fire spots from January 2016 to January 2017 over Thailand, which was downloaded from Moderate Resolution Imaging Spectroradiometer (MODIS) provided by NASA's Fire Information for Resource Management System (FIRMS).

References:

Andreae, M. O., and Gelencsér, A.: Black carbon or brown carbon? The nature of light-absorbing carbonaceous

aerosols, Atmos. Chem. Phys., 6, 3131-3148, https://doi.org/10.5194/acp-6-3131-2006, 2006.

Babar, Z. B., Park, J.-H., and Lim, H.-J.: Influence of NH_3 on secondary organic aerosols from the ozonolysis and photooxidation of α-pinene in a flow reactor, Atmos. Environ., 164, 71-84, https://doi.org/10.1016/j.atmosenv.2017.05.034, 2017.

Barnard, J. C., Volkamer, R., and Kassianov, E. I.: Estimation of the mass absorption cross section of the organic carbon component of aerosols in the Mexico City Metropolitan Area, Atmos. Chem. Phys., 8, 6665-6679, http://doi.org/10.5194/acp-8-6665-2008, 2008.

Bond, T. C., and Bergstrom, R. W.: Light Absorption by Carbonaceous Particles: An Investigative Review, Aerosol Sci. Technol., 40, 27-67, https://doi.org/10.1080/02786820500421521, 2006.

Chen, H., Liao, Z. L., Gu, X. Y., Xie, J. Q., Li, H. Z., and Zhang, J.: Anthropogenic Influences of Paved Runoff and Sanitary Sewage on the Dissolved Organic Matter Quality of Wet Weather Overflows: An Excitation-Emission Matrix Parallel Factor Analysis Assessment, Environ. Sci. Technol., 51, 1157-1167, https://doi.org/10.1021/acs.est.6b03727, 2017a.

Chen, Q., Ikemori, F., and Mochida, M.: Light Absorption and Excitation-Emission Fluorescence of Urban Organic Aerosol Components and Their Relationship to Chemical Structure, Environ. Sci. Technol., 50, 10859-10868, https://doi.org/10.1021/acs.est.6b02541, 2016a.

Chen, Q., Miyazaki, Y., Kawamura, K., Matsumoto, K., Coburn, S., Volkamer, R., Iwamoto, Y., Kagami, S., Deng, Y., Ogawa, S., Ramasamy, S., Kato, S., Ida, A., Kajii, Y., and Mochida, M.: Characterization of Chromophoric Water-Soluble Organic Matter in Urban, Forest, and Marine Aerosols by HR-ToF-AMS Analysis and Excitation-Emission Matrix Spectroscopy, Environ. Sci. Technol., 50, 10351-10360, https://doi.org/10.1021/acs.est.6b01643, 2016b.

Chen, Q., Ikemori, F., Nakamura, Y., Vodicka, P., Kawamura, K., and Mochida, M.: Structural and Light-Absorption Characteristics of Complex Water-Insoluble Organic Mixtures in Urban Submicrometer Aerosols, Environ. Sci. Technol., 51, 8293-8303, https://doi.org/10.1021/acs.est.7b01630., 2017b.

Chen, Q., Mu, Z., Song, W., Wang, Y., Yang, Z., Zhang, L., and Zhang, Y. L.: Size - Resolved Characterization of the Chromophores in Atmospheric Particulate Matter From a Typical Coal - Burning City in China, J. Geophys. Res.-Atmos., 124, 10546-10563, https://doi.org/10.1029/2019jd031149, 2019.

Chen, W., Westerhoff, P., Leenheer, J. A., and Booksh, K.: Fluorescence excitation - Emission matrix regional integration to quantify spectra for dissolved organic matter, Environ. Sci. Technol., 37, 5701-5710, https://doi.org/10.1021/es034354c, 2003.

Chen, Y., Ge, X., Chen, H., Xie, X., Chen, Y., Wang, J., Ye, Z., Bao, M., Zhang, Y., and Chen, M.: Seasonal light absorption properties of water-soluble brown carbon in atmospheric fine particles in Nanjing, China, Atmos. Environ., 230-240, https://doi.org/10.1016/j.atmosenv.2018.06.002, 2018.

Cheng, Y., He, K. B., Zheng, M., Duan, F. K., Du, Z. Y., Ma, Y. L., Tan, J. H., Yang, F. M., Liu, J. M., Zhang, X. L., Weber, R. J., Bergin, M. H., and Russell, A. G.: Mass absorption efficiency of elemental carbon and water-soluble organic carbon in Beijing, China, Atmos. Chem. Phys., 11, 11497-11510, https://doi.org/10.5194/acp-11-11497-2011, 2011.

Cheng, Y., He, K.-b., Du, Z.-y., Engling, G., Liu, J.-m., Ma, Y.-l., Zheng, M., and Weber, R. J.: The characteristics of

brown carbon aerosol during winter in Beijing, Atmos. Environ., 127, 355-364, https://doi.org/10.1016/j.atmosenv.2015.12.035, 2016.

Dasari, S., Andersson, A., Bikkina, S., Holmstrand, H., Budhavant, K., Satheesh, S. K., Asmi, E., Kesti, J., Backman, J., and Salam, A.: Photochemical degradation affects the light absorption of water-soluble brown carbon in the South Asian outflow, Sci. Adv., 5, https://doi.org/10.1126/sciadv.aau8066, 2019.

Fan, X., Wei, S., Zhu, M., Song, J., and Peng, P. a.: Comprehensive characterization of humic-like substances in smoke PM2.5 emitted from the combustion of biomass materials and fossil fuels, Atmos. Chem. Phys., 16, 13321-13340, https://doi.org/10.5194/acp-16-13321-2016, 2016.

Fan, X., Li, M., Cao, T., Cheng, C., Li, F., Xie, Y., Wei, S., Song, J., and Peng, P. a.: Optical properties and oxidative potential of water- and alkaline-soluble brown carbon in smoke particles emitted from laboratory simulated biomass burning, Atmos. Environ., 194, 48-57, https://doi.org/10.1016/j.atmosenv.2018.09.025, 2018.

Gao, Y., and Zhang, Y.: Formation and photochemical investigation of brown carbon by hydroxyacetone reactions with glycine and ammonium sulfate, RSC Advances, 8, 20719-20725, https://doi.org/10.1039/c8ra02019a, 2018.

Hoffer, A., Gelencsér, A., Guyon, P., Kiss, G., Schmid, O., Frank, G., Artaxo, P., and Andreae, M.: Optical properties of humic-like substances (HULIS) in biomass-burning aerosols, Atmos. Chem. Phys., 6, 3563-3570, https://doi.org/10.5194/acp-6-3563-2006, 2006.

Lee, H. J., Aiona, P. K., Laskin, A., Laskin, J., and Nizkorodov, S. A.: Effect of solar radiation on the optical properties and molecular composition of laboratory proxies of atmospheric brown carbon, Environ. Sci. Technol., 48, 10217-10226, https://doi.org/10.1021/es502515r, 2014.

Liu, C., Chung, C. E., Yin, Y., and Schnaiter, M.: The absorption Ångström exponent of black carbon: from numerical aspects, Atmos. Chem. Phys., 18, 6259-6273, https://doi.org/10.5194/acp-18-6259-2018, 2018a.

Liu, J., Bergin, M., Guo, H., King, L., Kotra, N., Edgerton, E., and Weber, R. J.: Size-resolved measurements of brown carbon in water and methanol extracts and estimates of their contribution to ambient fine-particle light absorption, Atmos. Chem. Phys., 13, 12389-12404, https://doi.org/10.5194/acp-13-12389-2013, 2013.

Liu, J., Mo, Y., Ding, P., Li, J., Shen, C., and Zhang, G.: Dual carbon isotopes (^{14}C and ^{13}C) and optical properties of WSOC and HULIS-C during winter in Guangzhou, China, Sci. Total Environ., 633, 1571-1578, https://doi.org/10.1016/j.scitotenv.2018.03.293, 2018b.

Mo, Y., Li, J., Jiang, B., Su, T., Geng, X., Liu, J., Jiang, H., Shen, C., Ding, P., Zhong, G., Cheng, Z., Liao, Y., Tian, C., Chen, Y., and Zhang, G.: Sources, compositions, and optical properties of humic-like substances in Beijing during the 2014 APEC summit: Results from dual carbon isotope and Fourier-transform ion cyclotron resonance mass spectrometry analyses, Environ. Pollut., 239, 322-331, https://doi.org/10.1016/j.envpol.2018.04.041, 2018.

Murphy, K. R., Stedmon, C. A., Wenig, P., and Bro, R.: OpenFluor– an online spectral library of auto-fluorescence by organic compounds in the environment, Anal. Methods, 6, 658-661, https://doi.org/10.1039/c3ay41935e, 2014.

Park, S. S., and Yu, J.: Chemical and light absorption properties of humic-like substances from biomass burning emissions under controlled combustion experiments, Atmos. Environ., 136, 114-122, https://doi.org/10.1016/j.atmosenv.2016.04.022, 2016.

Pohlker, C., Huffman, J. A., and P?schl, U.: Autofluorescence of atmospheric bioaerosols – fluorescent biomolecules

and potential interferences, Atmos. Meas. Tech., 5, 37-71, https://doi.org/10.5194/amt-5-37-2012, 2012.

Qin, J., Zhang, L., Zhou, X., Duan, J., Mu, S., Xiao, K., Hu, J., and Tan, J.: Fluorescence fingerprinting properties for exploring water-soluble organic compounds in $PM_{2.5}$ in an industrial city of northwest China, Atmos. Environ., 184, 203-211, https://doi.org/10.1016/j.atmosenv.2018.04.049, 2018.

Shetty, N. J., Pandey, A., Baker, S., Hao, W. M., and Chakrabarty, R. K.: Measuring light absorption by freshly emitted organic aerosols: optical artifacts in traditional solvent-extraction-based methods, Atmos. Chem. Phys., 19, 8817-8830, https://doi.org/10.5194/acp-19-8817-2019, 2019.

Stedmon, C. A., and Markager, S.: Resolving the variability in dissolved organic matter fluorescence in a temperate estuary and its catchment using PARAFAC analysis, Limnol. Oceanogr., 50, 686-697, https://doi.org/10.4319/lo.2005.50.2.0686, 2005.

Tang, J., Li, J., Mo, Y., Safaei Khorram, M., Chen, Y., Tang, J., Zhang, Y., Song, J., and Zhang, G.: Light absorption and emissions inventory of humic-like substances from simulated rainforest biomass burning in Southeast Asia, Environ. Pollut., 262, 114266, https://doi.org/10.1016/j.envpol.2020.114266, 2020a.

Tang, J., Li, J., Su, T., Han, Y., Mo, Y., Jiang, H., Cui, M., Jiang, B., Chen, Y., Tang, J., Song, J., Peng, P., and Zhang, G.: Molecular compositions and optical properties of dissolved brown carbon in biomass burning, coal combustion, and vehicle emission aerosols illuminated by excitation–emission matrix spectroscopy and Fourier transform ion cyclotron resonance mass spectrometry analysis, Atmos. Chem. Phys., 20, 2513-2532, https://doi.org/10.5194/acp-20-2513-2020, 2020b.

Wang, J., Jiang, H., Jiang, H., Mo, Y., Geng, X., Li, J., Mao, S., Bualert, S., Ma, S., Li, J., and Zhang, G.: Source apportionment of water-soluble oxidative potential in ambient total suspended particulate from Bangkok: Biomass burning versus fossil fuel combustion, Atmos. Environ., 235, 117624, https://doi.org/10.1016/j.atmosenv.2020.117624, 2020.

Wu, G., Ram, K., Fu, P., Wang, W., Zhang, Y., Liu, X., Stone, E. A., Pradhan, B. B., Dangol, P. M., Panday, A. K., Wan, X., Bai, Z., Kang, S., Zhang, Q., and Cong, Z.: Water-Soluble Brown Carbon in Atmospheric Aerosols from Godavari (Nepal), a Regional Representative of South Asia, Environ. Sci. Technol., 53, 3471-3479, https://doi.org/10.1021/acs.est.9b00596, 2019.

Wünsch, U. J., Bro, R., Stedmon, C. A., Wenig, P., and Murphy, K. R.: Emerging patterns in the global distribution of dissolved organic matter fluorescence, Anal. Methods, 11, 888-893, https://doi.org/10.1039/c8ay02422g, 2019.

Xie, C., Xu, W., Wang, J., Wang, Q., Liu, D., Tang, G., Chen, P., Du, W., Zhao, J., Zhang, Y., Zhou, W., Han, T., Bian, Q., Li, J., Fu, P., Wang, Z., Ge, X., Allan, J., Coe, H., and Sun, Y.: Vertical characterization of aerosol optical properties and brown carbon in winter in urban Beijing, China, Atmos. Chem. Phys., 19, 165-179, https://doi.org/10.5194/acp-19-165-2019, 2019a.

Xie, M., Chen, X., Holder, A. L., Hays, M. D., Lewandowski, M., Offenberg, J. H., Kleindienst, T. E., Jaoui, M., and Hannigan, M. P.: Light absorption of organic carbon and its sources at a southeastern U.S. location in summer, Environ. Pollut., 244, 38-46, https://doi.org/10.1016/j.envpol.2018.09.125, 2019b.

Yan, C., Zheng, M., Sullivan, A. P., Bosch, C., Desyaterik, Y., Andersson, A., Li, X., Guo, X., Zhou, T., Gustafsson, Ö., and Collett, J. L.: Chemical characteristics and light-absorbing property of water-soluble organic carbon in

Beijing: Biomass burning contributions, Atmos. Environ., 121, 4-12, https://doi.org/10.1016/j.atmosenv.2015.05.005, 2015.

Zhou, Y., Wen, H., Liu, J., Pu, W., Chen, Q., and Wang, X.: The optical characteristics and sources of chromophoric dissolved organic matter (CDOM) in seasonal snow of northwestern China, The Cryosphere, 13, 157-175, https://doi.org/10.5194/tc-13-157-2019, 2019.